PUBLICATIONS OF THE ASTRONOMICAL SOCIETY OF THE PACIFIC, **117**:1021–1048, 2005 October
© 2005. The Astronomical Society of the Pacific. All rights reserved. Printed in U.S.A.

Review

Astrometric Methods and Instrumentation to Identify and Characterize Extrasolar Planets: A Review

ALESSANDRO SOZZETTI[1,2]
Received 2005 March 23; accepted 2005 July 5; published 2005 September 22

ABSTRACT. I present a review of astrometric techniques and instrumentation used to search for, detect, and characterize extrasolar planets. First, I briefly summarize the properties of the current sample of extrasolar planets, in connection with predictions from theoretical models of planet formation and evolution. Next, the generic approach to planet detection with astrometry is described, with significant discussion of a variety of technical, statistical, and astrophysical issues to be faced by future ground-based and space-borne efforts in order to achieve the required degree of measurement precision. After a brief summary of past and present efforts to detect planets via milliarcsecond astrometry, I then discuss the planet-finding capabilities of future astrometric observatories aiming at microarcsecond precision. Finally, I outline a number of experiments that can be conducted by means of high-precision astrometry during the next decade, to illustrate its potential for important contributions to planetary science, compared to other indirect and direct methods for the detection and characterization of planetary systems.

1. INTRODUCTION

The astrophysics of planetary systems is a good example of a branch of science in which theory is mostly driven by observations. Hardly any of the properties of the sample of ~150 extrasolar giant planets discovered to date[3] (Jupiters on orbits of a few days; very high eccentricities; objects with masses 5 to 10 times that of Jupiter) had been predicted a priori by theoretical models. Correlations among planetary orbital and physical parameters had not been anticipated. The dependence of the frequency and properties of planetary systems on some of the characteristics of the parent stars (mass and metallicity) had not been foreseen.

The unexpected properties of extrasolar planets have sparked new enthusiasm among theorists, who have engaged in fruitful intellectual confrontations, with the aim of moving from a set of models separately describing different aspects of the physics of the formation and evolution of planetary systems to a plausible, unified theory capable of making robust and testable predictions. Furthermore, a number of new and old techniques of astronomy have been energized by the new discoveries, with the twin goals of following up and better characterizing the extrasolar planet sample, and covering new areas of the discovery space. The result is an ongoing, positive, creative tension between theory and observation that will put to the test the most basic ideas of how planets form and evolve.

Among detection techniques, astrometry is the oldest. Nonetheless, no planet discovery announcement has been ascribed to it yet; only a few confirmations of previously detected systems have made the news well after other novel methods, considered completely unrealistic a few years back, had already achieved important results. However, the contribution of astrometric measurements of sufficient precision is potentially very relevant to a continued improvement of our understanding of the formation and evolution of planetary systems, and possibly for the identification of the first Earth-sized objects worthy of follow-up observations to search for signs of the presence of essential "biomarkers" (i.e., of the existence of life as we know it outside of our solar system).

It is the aim of this review paper to describe the current and future sensitivity of astrometric measurements, both from the ground and in space, and to delineate the areas of planetary science in which astrometry will be able to make significant contributions compared to other direct and indirect methods for the detection and characterization of planetary systems. In § 2 I summarize the observed properties of extrasolar planets, in connection with renewed theoretical efforts in the fields of planet formation and evolution. I describe in § 3 the astrometric methods and instrumentation used to hunt for planets, in light of a number of technological and astrophysical challenges to be faced in order to achieve the required degree of measurement

[1] Department of Physics and Astronomy, University of Pittsburgh, Pittsburgh, PA 15260.

[2] Smithsonian Astrophysical Observatory, Harvard-Smithsonian Center for Astrophysics, 60 Garden Street, Cambridge, MA 02138; asozzetti@cfa.harvard.edu.

[3] See for example the continuously updated Extrasolar Planet Encyclopedia Web site (http://www.obspm.fr/encycl/encycl.html), and references to published papers therein. Objects with masses M_p below the Deuterium-burning threshold of $\approx 13 M_J$ (where M_J is the mass of Jupiter; Oppenheimer et al. 2000) are defined as planets and included in the catalog, with the exception of companions with masses as large as 20 M_J in systems already containing one planetary-mass companion.

precision. Section 4 contains a brief review of past and present efforts to detect planets with astrometry. In § 5 I discuss the planet-finding capabilities of future astrometric observatories. Finally, in § 6 I outline a number of experiments that can be conducted with high-precision astrometry, to illustrate its potential for important contributions to planetary science.

2. EMERGING STATISTICAL PROPERTIES OF PLANETARY SYSTEMS

Ten years after the announcement of the first Jupiter-sized object orbiting a star other than the Sun (Mayor & Queloz 1995), the number of extrasolar planets announced has increased by a few tens per year. Based on the large data sets mostly made available by ground-based Doppler surveys (e.g., Marcy et al. 2004b and references therein; Mayor et al. 2004 and references therein), estimates of the frequency f_p of giant planets around solar-type (late F, G, and early K spectral types) stars in the solar neighborhood ($D \lesssim 50$ pc) are all in fair agreement with each other (Zucker & Mazeh 2001a; Tabachnik & Tremaine 2002; Lineweaver & Grether 2003; Marcy et al. 2004b; Naef et al. 2005). Quoted values range between $f_p \simeq 4\%$–5% and $f_p \simeq 6\%$–9% for planet masses in the range $1M_J \leq M_p \leq 10M_J$ and orbital radii $a \leq 3$ AU, and $0.5M_J \leq M_p \leq 10M_J$ and $a \leq 4$ AU, respectively.

On the observational side, the startling diversity of planetary systems, when compared with the properties of our own solar system, has, if possible, become more evident with the newly discovered planets. On the theoretical side, the only concept that has not yet undergone significant revision or criticism is the paradigmatic statement that planets form within gaseous disks around young T Tauri stars. Many old ideas have been revisited or revived, and a number of completely new ones have been proposed in an attempt to confront and explain the observational data on extrasolar planets.

2.1. Mass, Period, and Eccentricity Distributions

The extrasolar planet sample exhibits many interesting and surprising characteristics. The distribution of minimum masses[4] rises toward lower masses (e.g., Tabachnik & Tremaine 2002 and references therein; Lineweaver & Grether 2003; Marcy et al. 2004a). Incompleteness below $M_p \sin i \sim 0.5M_J$ becomes increasingly important, although recently, objects with minimum masses as low as the mass of Neptune have been discovered (Butler et al. 2004; McArthur et al. 2004; Santos et al. 2004b). The sharp cutoff at the high-mass tail of the distribution, above $M_p \sin i \sim 10$–$15M_J$, with very few low-mass companions to solar-type stars in the range $10M_J \lesssim M_p \sin i \lesssim 80M_J$, and for orbital periods up to a decade, is often referred to as the "brown dwarf desert."

[4] Only the product $M_p \sin i$ between the actual companion mass and the unknown inclination of the orbital plane with respect to the line of sight can be derived from Doppler-shift measurements.

Theoretical predictions of the mass distribution of extrasolar planets within the context of the core-accretion model (e.g., Lissauer 1993; Pollack et al. 1996) of giant planet formation have recently been proposed (Alibert et al. 2005; Ida & Lin 2004a, 2005), which qualitatively reproduce the observed one (particularly for objects with $M_p \lesssim 5M_J$). Rice et al. (2003c) and Rafikov (2005) argue instead that giant planets formed by disk instability (e.g., Boss 1997, 2001, 2004; Mayer et al. 2002) should preferentially populate the high-mass tail ($M_p \gtrsim 5M_J$) of the planet mass distribution, while Mayer et al. (2004) indicate the possibility that the range of masses of giant planets formed via core accretion and disk instability could significantly overlap.

The period (P) and eccentricity (e) distributions also contain interesting features (Tabachnik & Tremaine 2002 and references therein; Udry et al. 2003; Marcy et al. 2004a; Halbwachs et al. 2005). Orbital periods are found in the range $1.5 \lesssim P \lesssim 5400$ days. About 20% of the planet sample, the so-called "hot" Jupiters, are found orbiting within 0.1 AU. The number of planets increases with orbital period for $60 \lesssim P \lesssim 2000$ days, with increasing incompleteness for orbital radii $\gtrsim$3 AU. The median of the eccentricity distribution of extrasolar planets is ~0.3. The orbits of extrasolar planets span the whole range of available eccentricities, and they can be extremely elongated (Naef et al. 2001). Planets orbiting within 0.1 AU are all found with $e \simeq 0.0$, a feature usually explained in terms of tidal circularization (Goldreich & Soter 1966).

Predictions regarding the actual orbital distance distribution of giant planets have been made within the context of core-accretion models that include mechanisms of inward orbital migration due to tidal interactions between a gaseous disk and an embedded planet (e.g., Goldreich & Tremaine 1979, 1980; Lin & Papaloizou 1993; Ward 1986, 1997). Trilling et al. (2002) and Armitage et al. (2002) were able to qualitatively reproduce the observed semimajor axis distribution of giant planets for $a > 0.1$ AU. Similar results were obtained recently by Alibert et al. (2004, 2005) and by Ida & Lin (2004a, 2005). However, these models largely neglect the difficult problem of identifying general mechanisms capable of stopping orbital migration (e.g., Terquem 2003 and references therein). In the context of the disk instability model of giant planet formation, migration efficiency might not be very effective (Rice et al. 2003a, 2003c; Mayer et al. 2004); thus, planets formed by this mechanism should be found on not too close-in orbits (Rice et al. 2003c; Rafikov 2005).

The large spread of orbital eccentricities is difficult to explain by the standard core-accretion model. Several mechanisms have been proposed to reproduce the observed e-distribution, which are based on dynamical interactions of various nature, such as interactions between the planet and a gaseous or planetesimal disk, planet-planet resonant interactions, close encounters between planets, or secular interactions with a distant companion star (for a review, see Tremaine & Zakamska 2004 and ref-

erences therein), but none of them can alone represent the observed distribution in a natural way. Furthermore, in multiple-planet systems, different eccentricity excitation mechanisms induce different evolution of the orbital alignment, and planetary orbits could be significantly noncoplanar. The alternative mode of planet formation by disk instability gives rise to eccentric orbits, but no clear prediction of the final distribution of eccentricities has been provided yet (e.g., Papaloizou & Terquem 2001; Terquem & Papaloizou 2002; Mayer et al. 2004).

2.2. Correlations

With improved statistics, in recent years a number of studies have been carried out to find evidence of correlations among orbital parameters and masses and between planet characteristics and stellar host properties.

As initially pointed out by Zucker & Mazeh (2002), Udry et al. (2003), and more recently by Eggenberger et al. (2004), the extrasolar planet sample exhibits a statistically significant lack of massive, close-in planets. These objects are the easiest to detect with the Doppler method;[5] thus, the paucity of high-mass planets on short-period orbits is real, and not due to selection effects.

Regardless of the formation mode, orbital migration effects are likely responsible for the observed $M_p \sin i$–P correlation. Many models can reproduce such results, including reduced migration efficiency due to gap opening (Ward 1997; Trilling et al. 2002), substantial mass loss through Roche lobe overflow (Trilling et al. 1998; Gu et al. 2003), and accelerated orbital decay due to enhanced tidal interactions with the host stars (Pätzold & Rauer 2002). Finally, Ida & Lin (2004a) have derived a theoretical mass-period diagram that closely resembles that of the extrasolar planet sample, and predicted a paucity of planets in the intermediate-mass range $0.05 \leq M_p \leq 0.5 M_J$, for orbital distances <3 AU.

The possibility that supersolar metallicity could correspond to a higher likelihood of a given star harboring a planet has been the subject of a large number of studies (for a detailed review, see Gonzalez 2003). Recent works (e.g., Santos et al. 2001, 2004a; Fischer & Valenti 2005) have conclusively shown that planet occurrence correlates strongly with the host stars' primordial metallicity. Up to ~20% of metal-rich ([Fe/H] $\gtrsim 0.3$) F-G-K stars harbor planets, while less than 3% of metal-poor stars ([Fe/H] $\lesssim 0.0$) have been found to be planet hosts.

Based on the core accretion model, Kornet et al. (2005) and Ida & Lin (2004b) have quantified the dependence of planetary frequency on stellar metallicity, in qualitatively good agreement with the observed trend. The alternative scenario of giant planet formation via disk instability, however, is mostly insensitive to the primordial metal content of the protoplanetary disk (Boss 2002; Rice et al. 2003c); thus, planet occurrence should not be hampered around metal-poor stars. The observed trend suggests that giant planet formation by core accretion predominates in the metal-rich regime ([Fe/H] $\simeq 0.0$). However, due to the low numbers of metal-poor stars ([Fe/H] $\lesssim -0.5$) surveyed to date, no definitive conclusion can be drawn, except that maybe both mechanisms operate (Beer et al. 2004).

Several authors have in the past searched for possible correlations between stellar metallicity and planet properties. Udry et al. (2002), Santos et al. (2001, 2003), and Fischer et al. (2002) searched for correlations in the $M_p \sin i$-[Fe/H] and e-[Fe/H] diagrams, but concluded that no statistically significant trend can be found. The P-[Fe/H] diagram deserves instead more attention. Gonzalez (1998) and Queloz et al. (2000) initially argued that metal-rich stars seem to possess an excess of very short period planets with respect to other planet hosts. In later works (Santos et al. 2001, 2003; Laws et al. 2003), no trend was found. However, after removing some potential sources of bias, Sozzetti (2004) has shown how this trend is still present in the data, specifically when one restricts the analysis to single planets orbiting single stars.

If real, the P-[Fe/H] correlation could reflect the fact that migration rates are slowed down in metal-poor protoplanetary disks (Livio & Pringle 2003), or it might be indicative of longer timescales for giant planet formation around metal-poor stars, and thus reduced migration efficiency before the disk dissipates (Ida & Lin 2004a).

Finally, planet frequency appears to correlate with the primary mass. In particular, as pointed out by, e.g., Butler et al. (2004), the occurrence rate of giant planets orbiting within 2 AU around M dwarfs ($0.3\ M_\odot \lesssim M_* \lesssim 0.6\ M_\odot$) seems suppressed by about an order of magnitude with respect to that of analogous planets around F- and G-type dwarfs ($0.8\ M_\odot \lesssim M_* \lesssim 1.3\ M_\odot$).

The current small number of giant planets discovered around M dwarfs might still be partly an artifact due to the small-number statistics (Butler et al. 2004). However, the observed trend is supported by theoretical arguments (Laughlin et al. 2004; Ida & Lin 2005) for a strong dependence of planet occurrence rates on stellar mass, highlighted by a significantly suppressed probability of forming giant planets by core accretion around M dwarfs, and by an enhanced likelihood for M dwarfs to harbor Neptune-sized objects. Planet occurrence, on the other hand, may not be a strong function of the primary mass for objects formed by disk instability (e.g., Boss 2000).

2.3. Multiple Systems and Planets in Stellar Systems

Some 10% of planet hosts are found to be orbited by multiple systems containing up to four planets, while ~12% of the planet-bearing stars are themselves components of wide multiple stellar systems, and in two of the latter cases the stars harbor multiple-planet systems.

A few authors have searched for differences between the distributions of orbital elements and masses of planets orbiting

[5] Recall that the radial velocity amplitude $K \propto P^{-1/3} M_p \sin i$.

single and multiple stars and single- and multiple-planet systems. Zucker & Mazeh (2002) and Eggenberger et al. (2004) presented evidence for no correlation between masses and periods of planets found in stellar systems, while Marcy et al. (2004a) visually compared the eccentricity and mass distributions of single planets and planetary systems and concluded that no significant difference was apparent. Finally, Mazeh & Zucker (2003) have recently presented arguments for a correlation between mass ratios and period ratios among pairs of planets in multiple systems (assuming coplanarity of the orbits).

From a theoretical viewpoint, the overall impact of the presence of a secondary star on the efficiency of planet formation and migration is far from clear. For example, Nelson (2000) and Mayer et al. (2005) argue that giant planet formation by either core accretion or disk instability can be strongly inhibited in relatively close binary systems with separations of an order of a few tens of AUs. Boss (1998), however, comes to opposite conclusions. Due to enhanced migration and gas accretion rates (Kley & Burkert 2000; Kley 2000, 2001; Nelson 2003), planets formed around binaries should not show evidence for a mass-period correlation. These predictions appear to agree with the observed trend.

Theoretical investigations of the long-term dynamical evolution of multiple-planet systems (e.g., Kiseleva-Eggleton et al. 2002; Ji et al. 2003 and references therein; Correia et al. 2005; Barnes & Quinn 2004; Goździewski & Konacki 2004 and references therein) have pompted the division of such systems into three broad classes: (1) "hierarchical" planetary systems, with widely separated orbits, in which dynamical interactions appear negligible, (2) planetary systems subject to strong secular interactions, and (3) planetary systems locked in mean motion resonances, which in some cases exhibit important variations of the orbital elements on timescales comparable to the time span of the radial velocity monitoring. In multiple-planet systems, regions of dynamical stability do exist inside the parent stars' habitable zones,[6] where Earth-sized planets may be found (e.g., Menou & Tabachnik 2003 and references therein; Jones et al. 2005 and references therein). Furthermore, the detected giant planets in binaries are likely to reside in stable orbital configurations, and there are margins for the presence of rocky planets in the habitable zone of close binaries (e.g., Holman & Wiegert 1999; Pilat-Lohinger et al. 2003 and references therein; Marzari et al. 2005; Musielak et al. 2005 and references therein), although the formation of terrestrial planets in such environments does not easily occur in the first place (Thébault et al. 2002; Raymond & Barnes 2005; Barnes & Raymond 2004; Raymond et al. 2004). However, the lack of information on the actual mutual inclination angles between pairs of planetary orbits somewhat limits the generality of these findings.

[6] The habitable zone of any star is defined as the range of orbital distances at which a potential water reservoir, the primary ingredient for the development of life as we know it, would be found in liquid form (e.g., Kasting et al. 1993).

2.4. Planetary Radii and Atmospheres

A handful of hot Jupiters ($P \lesssim 4$ days) have been discovered by means of photometric transit surveys (Udalski et al. 2002a, 2002b, 2003; Alonso et al. 2004) and confirmed by high-resolution spectroscopic measurements (Torres et al. 2004; Bouchy et al. 2004; Moutou et al. 2004; Pont et al. 2004; Sozzetti et al. 2004; Konacki et al. 2003, 2004, 2005), while one, HD 209458b, was observed transiting (Charbonneau et al. 2000; Brown et al. 2001) subsequent to the detection of its gravitational pull on the star (Mazeh et al. 2000; Henry et al. 2000).

The combination of Doppler-shift and transit photometry measurements allows one to derive estimates of the true mass and radius of a planet. These two critically interesting parameters can then be used for directly constraining structural models of irradiated giant planets (see Guillot 2005 and references therein for a detailed review). The measured radii for six of the seven transiting planets provide good agreement with theoretical expectations, while all models seem to systematically underestimate the radius of HD 209458b. The recent successful detection of thermal emission in the infrared from the planet (Deming et al. 2005), and in particular the timing of the secondary eclipse, clearly suggests that the planet revolves on an orbit with no significant eccentricity, essentially ruling out mechanisms invoked to provide additional heat/power sources in the core, such as tidal dissipation of a nonzero eccentricity induced by the gravitational perturbation of an undetected long-period companion (Bodenheimer et al. 2001, 2003; Laughlin et al. 2005).

Transmission spectroscopy during transits has allowed for the detection of absorption features in the spectrum of HD 209458 that are indicative of the presence of various constituents in the planet's atmosphere, notably sodium, hydrogen, oxygen, and carbon (Charbonneau et al. 2002; Vidal-Madjar et al. 2003, 2004). Furthermore, the planet appears to have an extended atmosphere, presumably due to evaporation effects. In two cases, detection of the planet's thermal emission (Charbonneau et al. 2005; Deming et al. 2005) has permitted us to estimate the planets' effective temperatures and Bond albedos, and to infer the presence of atmospheric water vapor and carbon monoxide.

Theoretical predictions of the atmospheric composition, temperature, and circulation of irradiated giant planets (Burrows et al. 2005; Fortney et al. 2005; for a review, see Burrows 2005) are in fair agreement with the first infrared direct detections; however, a proper understanding of the fine details of the emergent spectra of TrES-1 and HD 209458b will require both improved modeling and larger, high-quality data sets. Finally, studies of the phenomenon of atmospheric escape from hot Jupiters (Lammer et al. 2003; Gu et al. 2003, 2004; Lecavelier des Etangs et al. 2004; Baraffe et al. 2004; Grießmeier et al. 2004) predict that under strong irradiation, these objects, depending on their mass and orbital distance, could undergo

significant evaporation of their gaseous envelope, in reasonable agreement with observations.

2.5. Toward a Unified Picture

The observational data on extrasolar planets show such striking properties that one must infer that planet formation and evolution is a very complex process. Indeed, the comparison between theory and observations indicates that there are numerous problems in connection with the elucidation of planetary formation and evolution processes.

An ideal theory of planet formation and evolution should be capable of explaining in a self-consistent way, be it deterministic or probabilistic, all the different properties of planetary systems discussed above. To this end, help from future data obtained with a variety of different techniques will be crucial. Ultimately, both theory and observation will have to provide answers to a number of fundamental questions, which can be summarized as follows. (1) Where are the earthlike planets, and what is their frequency? (2) What is the preferred method of gas giant planet formation? (3) Under which conditions does migration occur and stop? (4) What is the origin of the large planetary eccentricities? (5) Are multiple-planet orbits coplanar? (6) How many families of planetary systems can be identified from a dynamical viewpoint? (7) What are the atmospheres, inner structure, and evolutionary properties of gas giant planets? (8) Do stars with circumstellar dust disks actually shelter planets? (9) What are the actual mass and orbital element distributions of planetary systems? (10) How do planet properties and frequencies depend on the characteristics of the parent stars (spectral type, age, metallicity, and binarity/multiplicity)?

With the above questions in mind, I focus next on the potential contribution of astrometry from the ground and in space by presenting a summary of methods and instrumentation, by reviewing past and present efforts, by discussing future prospects, and by putting this technique into perspective with other planet detection methods.

3. ASTROMETRIC PLANET DETECTION TECHNIQUES

Astrometric detection of extrasolar planets can be conducted with instrumentation on the ground or in space. In this section I describe the generic approach to planet detection and measurement with astrometry, in terms of what type of data are needed, how to extract and model the planet signal from the data in the presence of a number of noise sources, and how to assess the significance of a detection. I conclude the section by summarizing results from a set of ground-based and spaceborne experiments aimed at demonstrating the theoretical predictions of the astrometric precision achievable under a variety of conditions.

The general analysis methods can be applied to astrometric observables appropriately defined for both monopupil and diluted-aperture telescopes, both from the ground and in space. To this end, I describe the techniques in terms of the basic observable and noise models and the estimation process. The observable model produces theoretical values for the data as a function of adjustable parameters. The noise model describes errors that corrupt the astrometric data. The estimation process finds parameter values that produce the closest agreement between the observable model estimates and the data, in light of the noise model.

3.1. Observable Model

The astrometric observable is generally defined as the angular position of a star as measured by a given instrument in its local frame of reference. The measurement could be, for example, intrinsically one-dimensional, as is the case for space missions such as ESA's *Hipparcos* (Perryman et al. 1997) and *Gaia* (Perryman et al. 2001), which are designed to perform angular position measurements in their sensitive directions by centroiding their diffraction-limited images. Or it could be a set of two coordinates on the focal plane of the instrument, as is the case for ground-based telescopes (e.g., Gatewood 1987; Dekany et al. 1994; Pravdo & Shaklan 1996). Finally, it could be the optical path-length difference between the two arms of an interferometer on the ground (Shao et al. 1988; Armstrong et al. 1998; Colavita et al. 1999; van Belle et al. 1998; Glindemann et al. 2003) or in space, such as NASA's *Space Interferometry Mission* (*SIM*; Danner & Unwin 1999), or the normalized difference between the signals of two photomultiplier tubes (the transfer function) of a space-borne interferometer, such as the *Hubble Space Telescope* fine guidance sensor (*HST* FGS; Taff 1990).

Both from the ground and in space, astrometric measurements can be performed in wide-angle mode; i.e., relative to a local frame of reference composed of a set of one or more reference stars at typical angular distances of several degrees from the target object. If the selected local reference frame lies at $\lesssim 1^\circ$, the data are said to be collected while operating in narrow-angle mode. From space, without the limiting presence of atmospheric turbulence, which induces large-scale wavefront distortions (Lindegren 1980), the astrometric observable can be determined with respect to a global inertial reference frame by accurately bridging together multi-epoch observations of objects distributed everywhere in the sky (and thus separated by typically tens of degrees) and by adopting a global closure condition over the whole celestial sphere. The combination of such an observing scenario and data-reduction method is called the global astrometric mode (Kovalevsky 1980).

Regardless of the mode of operation and the instrument used to carry out the measurements, four categories of information should be identified for inclusion in the observable model used to calculate theoretical values of the observable with negligible errors: (1) the location and motion of the target (if working in global astrometric mode) and a possible set of reference stars

(if working in wide-angle or narrow-angle mode), (2) the location and motion of the observing instrument (if on the ground) or the attitude of the spacecraft (if in space), (3) the number, masses, and orbital parameters of companions to the target (and reference stars, where applicable), and (4) any physical effects that modify the apparent positions of stars.

3.1.1. Stellar and Instrumental Parameters

The star information consists of the five basic astrometric parameters—position on the celestial sphere (two parameters, λ and β), proper motion (two parameters, μ_λ and μ_β), and parallax (one parameter, π)—plus the radial velocity v_r, which can be determined by auxiliary measurements or from a sufficiently large secular acceleration.

The stellar locations and motions are usually determined in the solar system barycentric frame in which the global frame is defined. A variety of transformations can be used to connect the instrument-specific observational frame to the stellar frame.

If the object's position in the instrument and barycentric frame are described by the vectors $\boldsymbol{Z}$ and $\boldsymbol{S}_*$, respectively, then for an all-sky survey instrument such as *Hipparcos* or *Gaia*, the mapping is specified by the 3×3 rotation matrix A:

$$\boldsymbol{Z} = A\boldsymbol{S}_*. \tag{1}$$

From this relation, the along-scan angular coordinate of the object, which constitutes the actual observable, can be solved for in terms of A and $\boldsymbol{S}_*$. The matrix A is a continuous function of time that specifies the spacecraft attitude. It could be defined by a set of nine functions $A_{ij}(t)$, $i, j = 1, 2, 3$. Or it could be expressed in terms of three Euler angles $[\phi(t), \theta(t), \psi(t)]$, as was done for *Hipparcos*. Alternatively, it could be described by means of the quaternion representation, as is currently envisioned for *Gaia*.

For an interferometer operating in wide-angle mode, both on the ground and in space, the measured optical path-length delay d_* corresponds to the instantaneous three-dimensional position of the target on the sky projected onto the interferometer baseline:

$$d_* = \boldsymbol{B} \cdot \boldsymbol{S}_* + C. \tag{2}$$

The baseline vector $\boldsymbol{B} = B\boldsymbol{u_b}$ of length B describes the spacecraft attitude, while C is a constant term representing residual internal optical path differences. In the narrow-angle regime, this expression is modified as:

$$\Delta d_{*,j} = \boldsymbol{B} \cdot (\boldsymbol{S}_* - \boldsymbol{S_j}). \tag{3}$$

The relative optical path-length delay $\Delta d_{*,j}$ is then the instantaneous angular distance between the target and its jth reference star projected onto $\boldsymbol{B}$. Due to the differential nature of the measurement, the constant term C cancels out, to first order.

Finally, in order to relate the detector frame of a ground-based monolithic telescope or *HST* FGS to the actual coordinates of an object in the sky, a plate-reduction transformation is applied (e.g., Kovalevsky & Seidelmann 2004). In this case, the two-dimensional standard Cartesian coordinate vector $\boldsymbol{s}(s_1, s_2)$ describing the position of the target in the plane of the sky is mapped into the two-dimensional vector of measured coordinates on the detector $\boldsymbol{r}(r_1, r_2)$ via the transformation

$$\boldsymbol{r} = M\boldsymbol{p}. \tag{4}$$

In the above expression, M is the model matrix:

$$M = \begin{pmatrix} s_1 & s_2 & 1 & 0 & 0 & 0 & \ldots \\ 0 & 0 & 0 & s_1 & s_2 & 1 & \ldots \end{pmatrix}. \tag{5}$$

The column vector $\boldsymbol{p} = (p_1, p_2, \ldots, p_n)$ contains the so-called plate constants. A minimum of six is required to describe scale and rotation factors and offsets of coordinate origins between the two frames of reference, but it is not uncommon to include focal plane tilt and other optical distortion terms, in addition to terms that are dependent on the magnitude and color index of the star observed. The same relation holds for all the objects used as reference stars.

3.1.2. Planet Parameters

Masses and orbits of companions to the target object (and reference stars, where applicable) come from fitting a model of Keplerian orbital motion to the data. The Keplerian orbit of each companion is described by seven parameters: semimajor axis a with respect to the center of mass of the system, period P, eccentricity e, inclination i, position angle of the line of nodes Ω, argument of pericenter ω, and epoch of pericenter passage τ.

The observable model computes the star's reflex motion projected onto the plane of the sky due to the gravitational pull of such companions, which might be stellar or substellar (brown dwarfs and planets) in nature. If the primary mass is M_* and the secondary is a planet of mass M_p, then assuming a perfectly circular orbit, the apparent amplitude of the perturbation (i.e., the stellar orbital radius around the center of mass of the system, scaled by the distance from the observer) is the so-called astrometric signature:

$$\alpha = \frac{M_p}{M_*}\frac{a}{D}. \tag{6}$$

If M_p and M_* are given in solar mass units, a in AU, and D in parsecs, then α is in arcseconds.

Table 1 summarizes the values of α for a range of planet masses at different orbital radii from a 1 $M_\odot$ star at 10 pc, compared to typical values of parallax and proper motion for stars in the solar neighborhood.

As one can see, planetary signatures are a higher order effect

TABLE 1
PARALLAX, PROPER MOTION, AND ASTROMETRIC SIGNATURES INDUCED BY PLANETS OF VARIOUS MASSES AND ORBITAL RADII

Source	α
Jupiter at 1 AU (μas)	100
Jupiter at 5 AU (μas)	500
Jupiter at 0.05 AU (μas)	5
Neptune at 1 AU (μas)	6
Earth at 1 AU (μas)	0.33
Parallax (μas)	1×10^5
Proper motion (μas yr^{-1})	5×10^5

NOTE.—A 1 $M_\odot$ star at 10 pc is assumed.

for astrometry. Jupiter-sized planets already produce perturbative effects whose size is smaller than the typical *Hipparcos* milliarcsecond (mas) measurement precision. Detection of orbital motion induced by terrestrial planets necessarily implies an improvement of 2–3 orders of magnitude in precision, down to the few microarcseond (μas) regime.

Finally, in the case of a multiple-planet system, for example, simply considering independent Keplerian orbits might not be sufficient whenever secular or resonant gravitational perturbations among planets in the systems (due to the presence of large mass ratios, highly eccentric orbits, commensurabilities between orbital periods, and significantly noncoplanar orbits) are strong enough to induce measurable variations of orbital elements over timescales comparable to the time span of observations. For these cases, additional information must be fed to the observable model, such as approximate analytical expressions describing the gravitational perturbations and consequent time variations of the orbital elements, or fully self-consistent fitting algorithms that include the direct solution of the equations of motion of an *N*-body system.

3.1.3. Physical Effects

A variety of physical effects that cause the apparent coordinates of observed stars to differ from the transformed values of their true barycentric coordinates can be taken into account in principle. In order to understand which effects are more relevant, the driver is the limiting single-measurement precision the adopted instrument is designed to achieve. The state-of-the-art astrometric precision of 1 mas has been set by *Hipparcos* and *HST* FGS. The expected improvement in measurement precision by a few orders of magnitude envisioned for future ground-based and space-borne instrumentation such as VLTI, Keck-I, *SIM*, and *Gaia* will sensibly increase the order of higher approximations.

Higher order perturbations can be classical in nature, such as additional secular variations in the target space motion with respect to the observer, or intrinsically relativistic, such as corrections to classical effects due to the motion of the observer itself, or contributions coming from the gravitational fields of

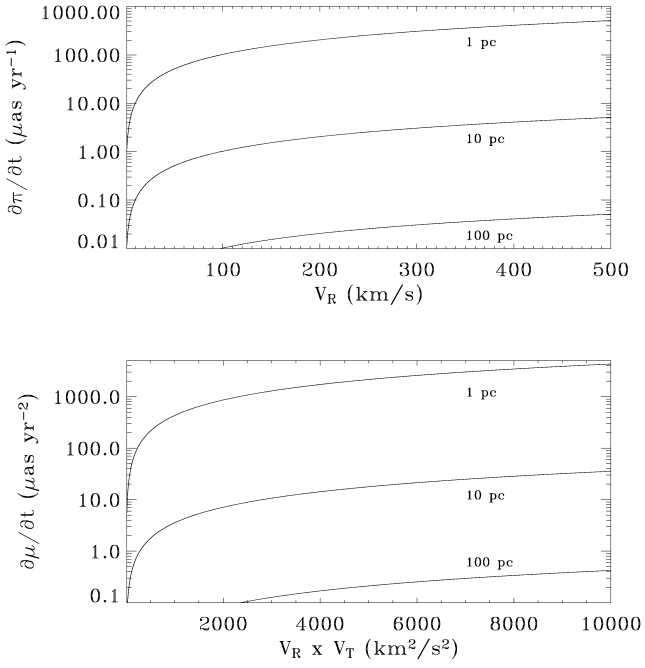

FIG. 1.—Magnitude of changing parallax and perspective acceleration as a function of stellar radial and tangential velocity.

massive bodies in the vicinity of the observer. Many of these effects are well known in pulsar timing work and are included in detailed models of pulse arrival times (e.g., Hellings 1986; Wolszczan & Frail 1992; Stairs et al. 1998, 2002 and references therein). However, they are often neglected in astrometric data reduction with mas-level precision.

Secular changes in proper motion (perspective acceleration) and annual parallax can be quantified as time derivatives of these two astrometric parameters (e.g., Dravins et al. 1999 and references therein):

$$\frac{d\mu}{dt} = -\frac{2v_r}{\mathrm{AU}}\,\mu\pi, \tag{7}$$

$$\frac{d\pi}{dt} = -\frac{v_r}{\mathrm{AU}}\,\pi^2. \tag{8}$$

The above quantities are expressed in arcsec yr^{-2} and arcsec yr^{-1}, respectively, if the radial velocity v_r is in km s^{-1}, π is in arcsec, μ is in arcsec yr^{-1}, and the astronomical unit AU $=$ 9.77792×10^5 arcsec km yr s^{-1}.

I show in Figure 1 the values of $d\mu/dt$ and $d\pi/dt$ as a function of v_r and of the product $v_t \times v_r$, where the tangential velocity $v_t = \mathrm{AU}\mu/\pi$ (with the astronomical unit now defined as AU $=$ 4.74 km yr s^{-1}). As one can see, the effect of changing annual parallax is below a few μas yr^{-1} for stars more distant than a few pc from the Sun, even assuming large values of v_r. Its inclusion in the observable model might then be limited

to the nearest stars. The contribution from perspective acceleration drops below a few μas yr^{-2} only for objects farther away than a few tens of pc; thus, such a corrective term might have to be taken into account in the observable model for a few hundred nearby, high-velocity stars.

Relativistic corrections to the motion of the observer with respect to the solar system barycenter (aberration) can be quantified through the formula (e.g., Klioner 2003; Kovalevsky & Seidelmann 2004)

$$\alpha_{\rm aberr} \simeq \frac{v}{c}\sin\vartheta - \frac{1}{4}\frac{v^2}{c^2}\sin 2\vartheta + \frac{1}{6}\frac{v^3}{c^3}\sin\vartheta(1+2\sin^2\vartheta) + O(c^{-4}), \quad (9)$$

where ϑ is the angular distance between the direction to the target and the observer's space velocity vector, v is the modulus of the space velocity vector of the observer, and c is the speed of light.

The magnitude of the classic aberration term (first order in v/c) is $\sim$20″–30″, while the second-order relativistic correction amounts to 1–3 mas. For a targeted measurement precision of 1 μas, terms of the order $(v/c)^3$ must be retained, but may be dropped for less stringent requirements. In addition, for relativistic stellar aberration to be properly accounted for, the spacecraft's velocity will need to be determined to an accuracy of 20 mm s^{-1} or better.

The purely general relativistic effect of deflection of light by solar system objects is instead defined by the expression (e.g., Klioner 2003)

$$\alpha_{\rm defl} = \frac{(1+\gamma)GM}{R_0 c^2}\cot\frac{\psi}{2}, \quad (10)$$

where ψ is the angular distance between the given solar system body and the source, G is the gravitational constant, R_0 is the distance between the observer and the Sun, M is the mass of the perturbing body, and $\gamma = 1$ is the post–post-Newtonian (PPN) parameter.

In Table 2 I summarize the magnitudes of the gravitational effects on limb-grazing light rays induced by all solar system planets and some of the largest moons. If the targeted measurement precision is of an order of 1–10 μas, the observable model should consider deflection by all these bodies when observing close to their directions, and even quadrupole effects induced by the nonoblateness of the major solar system planets may have to be considered (e.g., Klioner 2003).

Indeed, several attempts have been made in past years (Soffel 1989; Brumberg 1991; Klioner & Kopeikin 1992; de Felice et al. 1998, 2001, 2004; Vecchiato et al. 2003; Klioner 2003) to develop schemes for the reduction of astrometric observations at the μas precision level directly within the framework of general relativity, either employing nonperturbative approaches

TABLE 2
RELATIVISTIC LIGHT-DEFLECTION EFFECTS OF VARIOUS SOLAR SYSTEM OBJECTS

Source	α (μas)	$\delta_{\rm min}$ (1 μas)
Sun	1.75×10^6	180°
Mercury	83	9′
Venus	493	4.°5
Earth	574	178°/123°
Moon	26	9°/5°
Mars	116	25′
Jupiter	16,270	90°
Saturn	5780	17°
Uranus	2080	71′
Neptune	2533	51′
Ganymede	35	32″
Titan	32	14″
Io	31	19″
Callisto	28	23″
Europa	19	11″
Triton	10	0.″7
Pluto	7	0.″4

NOTE.—The post-Newtonian angular displacement α of a limb-grazing light ray due to the gravitational field of various solar system objects assumes the latter are perfect spheres. The angle $\delta_{\rm min}$ is the angular distance between the body and the light ray from a distant source at which the effect is still equal to 1 μas. For Earth and the Moon, two values are given, for a geostationary observer and for a satellite at a distance of 10^6 km from Earth.

or the PPN formulation (Will 1993). If a complete general relativistic observable model is implemented, other more subtle effects arise, such as the need to redefine parallax, proper motion, and radial velocity, depending on the given choice of the local reference system of the observer (whose motion must also be described in physically adequate relativistic terms; see, e.g., Klioner 2004) and the fact that these parameters, when higher order terms are included, can no longer be considered independent of each other. Furthermore, a number of possible effects that may be caused by gravitational fields produced outside of the solar system might have to be considered, such as weak gravitational lensing by distant sources (e.g., Belokurov & Evans 2002), binary systems viewed edge-on that contain compact objects such as neutron stars and/or black holes (Doroshenko & Kopeikin 1995), and gravitational waves (Kopeikin et al. 1999).

3.2. Noise Model

Astrometric data contain correlated and uncorrelated instrumental, atmospheric (if operating from the ground), and astrophysical noise. The noise model describes these uncertainties for use in the estimation process, which, particularly by taking into proper account correlated errors, provides the most accurate and sensitive results. When a noise source can be identified and modeled deterministically, e.g., a newly found com-

panion to a reference star, its predictable effects can be incorporated into the observable model, and any provision in the noise model is deleted. When uncertainties can be quantified but not modeled, they are accounted for in the noise model.

Below, I summarize a variety of known sources of astrometric noise. Where applicable (i.e., in the case of instrumental and atmospheric noise), the different implications for filled-aperture telescopes and interferometers are discussed separately. For instrumental noise, a further distinction is made depending on whether astrometric measurements are performed from the ground or in space. The relative importance of any given source of noise is gauged, bearing in mind the goal of achieving a final astrometric precision of an order of a few μas.

3.2.1. Instrumental Noise

The various sources of instrumental uncertainties in astrometric measurements can be described in terms of two general classes of error, random photon errors $\sigma_{\rm ph}$ and systematic errors $\sigma_{\rm sys}$.

The expression for the photometric noise of a monopupil telescope is (Lindegren 1978)

$$\sigma_{\rm ph} = \frac{\lambda}{4\pi A}\frac{1}{\rm S/N}, \tag{11}$$

where A is the telescope aperture and λ is the monochromatic wavelength of the observations (both in meters), while S/N is the signal-to-noise ratio of the target, including sky background and detector noise (S/N $\propto \sqrt{N} \propto \sqrt{t}$, where N is the number of photoelectrons and t is the exposure time in seconds). For a $m_v = 15$ solar-type star observed near the zenith with good (better than 0.″5) seeing conditions, and assuming an overall system efficiency $\varepsilon = 0.4$ (including CCD quantum efficiency and atmospheric and optics transmission), the contribution from $\sigma_{\rm ph}$ over small fields of view (<1′) can be ~300, ~30, and ~3 μas in 1 hr integration for $A = 1$, 10, and 100 m, respectively (see, e.g., Allen 2000).

For an interferometer, the photometric error is expressed as (Shao & Colavita 1992)

$$\sigma_{\rm ph} = \frac{\lambda}{2\pi B}\sqrt{\frac{t_c}{t}}\frac{1}{\rm S/N}, \tag{12}$$

with A replaced by B in equation (11). With average seeing conditions, the atmospheric coherence time t_c is typically a few tens of ms in the near-infrared K band (Shao & Colavita 1992; Quirrenbach et al. 1994; Lane & Colavita 2003), while the S/N per coherence time is a measure of the uncertainty σ_ϕ in the measurement of the phase of the interferometric fringes [$\sigma_\phi \approx ({\rm S/N})^{-1}$; see, e.g., Wyant 1975]. The value of S/N in this case is a function not only of the number of counts N, dark count and background, and read noise (as in the filled-aperture case), but also of the square of the complex visibility V^2 [S/N $\propto (NV^2)^{1/2}$; see, e.g., Quirrenbach et al. 1994; Colavita 1999].

If the interferometer sensitivity is limited by the actual atmospheric coherence time, accurate measurements of the fringe phase, and thus fringe tracking, can be performed only on very bright targets (typically $m_k \lesssim 5.0$) for which enough photons are collected in a coherence volume $t_c r_c^2$ (where r_c is the coherence diameter). When the interferometer is used in phase-referencing mode (e.g., Lane & Colavita 2003 and references therein), t_c can be artificially extended by more than an order of magnitude, thus allowing for an improvement of the limiting magnitude of the instrument, or allowing for a higher S/N at the same magnitude. The fundamental requirement is that the target and reference object be separated by less than an isoplanatic angle θ_i,[7] usually of an order of tens of arcseconds (e.g., Shao & Colavita 1992). The isoplanatic angle $\theta_i \propto r_c/h \propto \lambda^{6/5}$ (where h is the effective height of the turbulence profile; see, e.g., Colavita 1994); thus, as chances of finding reference objects are increased in larger fields, the obvious choice is to use the instrument in the infrared. However, it is with long baselines that interferometers have a major photon-noise advantage. For a $m_k = 13$ star, $B = 100$ m, S/N = 5, and $t_c = 100$ ms, then $\sigma_{\rm ph} \simeq 1$ μas in 1 hr integration can be achieved (e.g., Shao & Colavita 1992).

The instrumental systematic term for a monolithic telescope can, for example (Pravdo & Shaklan 1996), be expressed as

$$\sigma_{\rm sys} = \sqrt{\sigma_{\rm CCD}^2 + \sigma_{\rm OP}^2}. \tag{13}$$

The systematic limitations imposed by the CCD detectors (charge transfer efficiency, deviations from uniformity or from linear pixel response, etc.) through $\sigma_{\rm CCD}$ and optics imperfections (optical aberrations and distortions, pixellization, etc.) and through $\sigma_{\rm OP}$ can be overcome with improvements in image detector and optics technology. Centroid accuracies of 1/100 of a pixel are today readily achievable (Monet et al. 1992), translating into a typical value of $\sigma_{\rm CCD} \simeq 50$ μas. Future developments promise improvements of about 1 order of magnitude in CCD image location accuracy (Gai et al. 2001), with hopes to keep $\sigma_{\rm CCD} \lesssim 5$–10 μas. Optical aberrations and distortions for large apertures (>5 m) and small fields of view (<1′) are typically small. Pravdo & Shaklan (1996) have shown that for the Keck 10 m telescope, $\sigma_{\rm OP} \simeq 5$ μas or less.

For narrow-angle measurements with an interferometer, the systematic term will read (e.g., Shao & Colavita 1992)

$$\sigma_{\rm sys} = \sqrt{\sigma_{\rm l}^2 + \sigma_B^2}. \tag{14}$$

The two main sources of systematic errors arise from the uncertainty $\sigma_{\rm l} = \delta l/B$ with which optical delay lines in long-baseline interferometers can control internal optical path delays,

[7] The isoplanatic angle is the angle in the sky over which atmosphere-induced motion is well correlated.

and from the uncertainty regarding the interferometric baseline $\sigma_B = (\delta B/B)\vartheta$, where ϑ is the angular separation between the target and a reference star. As for the former, in order to reach a positional measurement precision of 10 μas with $B = 200$ m (the maximum baseline of the VLTI), measurements of optical paths must be made with an accuracy of $\sigma_l < 10$ nm, a challenging but not impossible achievement with today's technology (see, e.g., Shao et al. 1988). Due to the differential nature of the measurement, however, a knowledge of the instrument baseline does not need to be very precise. For $B = 200$ m and $\vartheta \approx 20''$, the goal of 10 μas precision is achieved by determining the baseline stability with an uncertainty of $\sigma_B \simeq 50$ μm, a requirement that is relaxed by a few orders of magnitude with respect to a wide-angle measurement (e.g., Shao et al. 1990).

Finally, if the astrometric measurements are performed in space, additional random and systematic error sources that are introduced by the satellite operations and environment must be taken into account. For example, a class of relevant error sources is related to the determination of the spacecraft attitude. Attitude errors can occur due to perturbations produced by the solar wind, micrometeorites, particle radiation, and radiation pressure. Thermal drifts and spacecraft jitter can also induce significant errors in attitude determination. However, these noise sources are hard to quantify a priori in a very general fashion. Detailed error models must be developed case by case (see § 4.5). Thus, in the design of a space-borne observatory for high-precision astrometry, whether a monolithic telescope or an interferometer, ad hoc calibration procedures must be devised in order to attain the goal of limiting the magnitude of such instrumental error sources at the few μas level.

3.2.2. Atmospheric Noise

For ground-based instrumentation, the atmosphere constitutes an additional source of noise through both its turbulent layers (a random component) and the differential chromatic refraction (DCR) effect (a systematic component).

The problems caused by the DCR effect can be very difficult to overcome. The magnitude of the effect depends on zenith distance z_0, air temperature and pressure, spectral band and star color, and even the nonsphericity of the Earth (e.g., Gubler & Tytler 1998). The precision of theoretical and empirical DCR correction formulae degrades very quickly with z_0. Even at small zenith distances, for a monolithic telescope, the goal of μas astrometry is unlikely to be attained. Typical uncertainties for small values of z_0 can be of an order of $\sigma_{\rm DCR} \approx 1$–3 mas and increase by over an order of magnitude close to the horizon (Kovalevsky & Seidelmann 2004).

For conventional narrow-angle astrometric measurements with separations of 10′–30′, the positional error $\sigma_{\rm atm}$ due to atmospheric turbulence is weakly dependent on separation and does not depend on A (or B). This prevents the achievement of submilliarcsecond astrometric precision (e.g., Lindegren 1980; Han 1989). For separations <1′–10′, the situation improves. In this regime, the astrometric error due to anisoplanatism for a filled-aperture telescope has been calculated in the past (Lindegren 1980; Shao & Colavita 1992) as

$$\sigma_{\rm atm} \approx 300 A^{-2/3} \vartheta t^{-1/2}, \tag{15}$$

where ϑ is in radians, A is expressed in meters, and the factor 300 is obtained directly from the phase-structure function describing the turbulence, assuming standard Kolmogorov-Hufnagel (Hufnagel 1974) atmospheric and wind-speed profiles for good seeing conditions (FWHM $\approx 0\farcs5$) typical of a site such as the Keck Observatory (e.g., Shao & Colavita 1992). The rather weak power dependency of $\sigma_{\rm atm}$ on target–reference star separation and objective diameter implies that a typical value of $\sigma_{\rm atm} \simeq 1$ mas is obtained with $A = 1$ m in $t = 1$ hr of integration, with a separation $\vartheta = 1'$. Suppressing $\sigma_{\rm atm}$ by 2 to 3 orders of magnitude would require unrealistically large A and t, unless ϑ is limited to uselessly small angles.

Interferometers can in principle get much closer to the limits in precision set by the atmosphere. For a diluted architecture, in fact, equation (15) now reads $\sigma_{\rm atm} \approx 300 B^{-2/3} \vartheta t^{-1/2}$. Values of B of an order of 100–200 m are more easily attainable than the equivalent filled-aperture size. Thus, for a 20″ star separation and a 200 m baseline, a 1 hr integration would allow one to achieve $\sigma_{\rm atm} \simeq 10$ μas (Shao & Colavita 1992). In conditions of extremely favorable seeing, large isoplanatic angles, and long atmospheric coherence times, such as those reported above Dome C in Antarctica (Lloyd et al. 2002; Lawrence et al. 2004), atmospheric errors in image motion may be reduced by another order of magnitude.

However, if phase referencing is used to artificially increase t_c and the limiting m_k, additional noise sources are introduced. In particular, coherence losses occur due to fluctuations in the fringe position during integration, which in turn induce visibility reduction by a factor $\eta = e^{-\sigma^2_{\Delta\phi}}$ (where $\sigma_{\Delta\phi}$ is a measure of jitter in the referenced phase; see, e.g., Colavita 1994). This in turn limits the achievable S/N in a given t_c, thus contributing to increase $\sigma_{\rm ph}$. These time-dependent effects can be divided into two classes, namely, instrument-specific errors in the determination of the phase, and those that are due to atmospheric propagation effects. The dominant effect (Quirrenbach et al. 1994) is again induced by DCR. For large values of z_0, $\eta \rightarrow 0$; thus, applications of this technique are likely to be restricted to moderate zenith angles, depending on wavelength and seeing.

3.2.3. Astrophysical Noise

While the abovementioned error sources can to some extent be dealt with and reduced, in order to progress toward the goal of a few μas precision, astrophysical noise sources (due to the environment or intrinsic to the target) cannot be easily minimized if present.

For example, Figure 2 shows a comparison between the

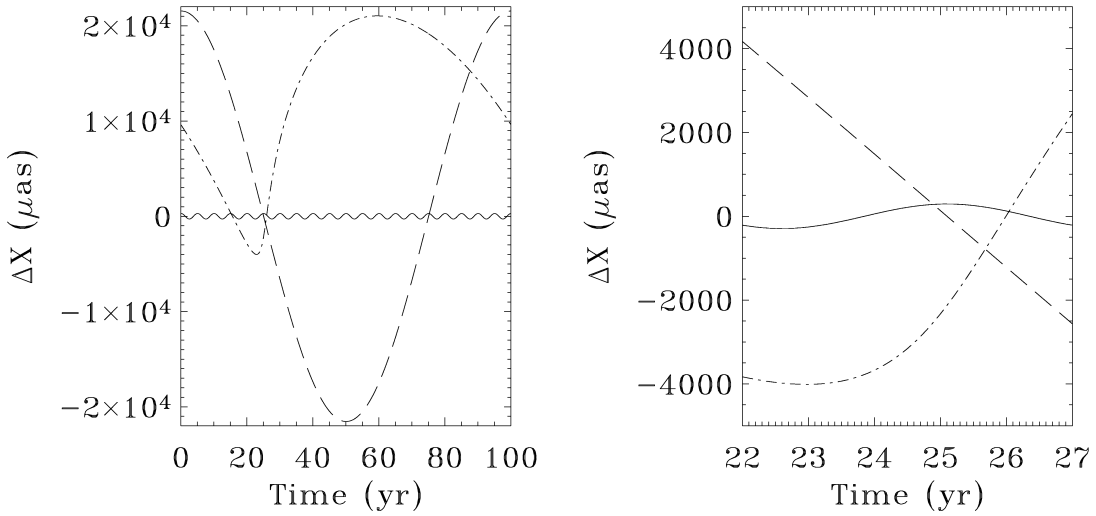

FIG. 2.—*Left*: Size of the gravitational perturbation along one axis, induced on a 1 M_* star at 100 pc by a $5M_J$ planet (*solid line*) with $P = 5$ yr, and a 0.1 $M_\odot$ star on a circular (*dotted line*) and eccentric ($e = 0.8$, *dash-dotted line*) orbit with $P = 100$ yr. *Right*: Zoomed-in region covering 5 years of observations.

gravitational perturbations (as seen along one of the two axes in the plane of the sky as a function of time) induced by a $5M_J$ and a 0.1 $M_\odot$ companion to a 1 $M_\odot$ star with periods of 5 and 100 yr, respectively, with the system at a distance $D = 100$ pc from the Sun. As one can see from the right panel of the figure, on a timescale that is short compared to the orbital period of the stellar companion, the astrometric signature of the planet is superposed to a large extent. The additional signal in the data could be easily misinterpreted as an extra proper motion component or as a significant acceleration, depending on the orbital characteristics of the long-period companion and epochs of observation.

As mentioned above, if the orbital characteristics of the perturbing stellar companion around a target and/or reference star(s) are known to exist in advance, they can be modeled within the context of the observable model. The dynamical effect of a previously unknown stellar companion otherwise constitutes a significant source of noise that might hamper the reliability of orbit reconstruction for a newly detected planet.

Such a problem will primarily affect future high-precision space-borne global astrometric missions such as *Gaia*, which will not have the luxury of preselecting the list of targets. In the case of relative astrometry, if feasible, one could require that the objects making up the local frame of reference not be orbited by stellar companions inducing unmodeled signatures larger than a few μas. A typical strategy to achieve this, adopted for example for the selection of the grid stars for *SIM*, is to look for reference objects that are K giants and preselect them on the basis of medium-precision radial velocity monitoring. In this case, the typically large distance of these stars (1 kpc) implies (provided they are not too faint; otherwise photon noise becomes an issue) a significant suppression of any astrometric signature that might significantly pollute the potential planetary signal from the target (e.g., Gould 2001 and references therein).

Another source of astrophysical noise due to the environment is the presence of a circumstellar disk. The motion of the center of mass of the disk, provoked by the excitation of spiral density waves by an embedded planet, induces an additional wobble in the stellar position, while time-variable, asymmetric starlight scattering by the disk can introduce shifts in the photocenter position.

Takeuchi et al. (2005) have recently studied these effects, assuming Jupiter-mass planets embedded in gravitationally stable circumstellar disks around young solar-type stars at the distance of the Taurus-Auriga star-forming region ($D \simeq 140$ pc). They conclude that the additional stellar motion that is caused dynamically by the disk's gravity is negligible (submicroarcsecond) with respect to the signature from the planet ($\sim$36 μas if the planet's semimajor axis is 5 AU). Variable disk illumination can induce peak-to-peak photocenter variations of an order of 10–100 μas, but they claim that *SIM* would not be sensitive to such excursions. Finally, Boss (1998) and Rice et al. (2003b) have quantified the magnitude of the astrometric displacement induced dynamically by a marginally unstable disk. They found that in this case the effect can be as large as 50–100 μas, but the typical timescale of this perturbation would be of an order of decades, as compared to a few years of observations with *SIM* or *Gaia*. Thus, such a source of astrometric noise should not constitute a major cause of concern.

The last important class of astrophysical noise sources that can cause shifts in the observed photocenter is not due to stellar environment, but rather is intrinsic to the target. Such noise sources include a variety of surface temperature inhomogeneities, such as spots and flares, and just like disks, they are

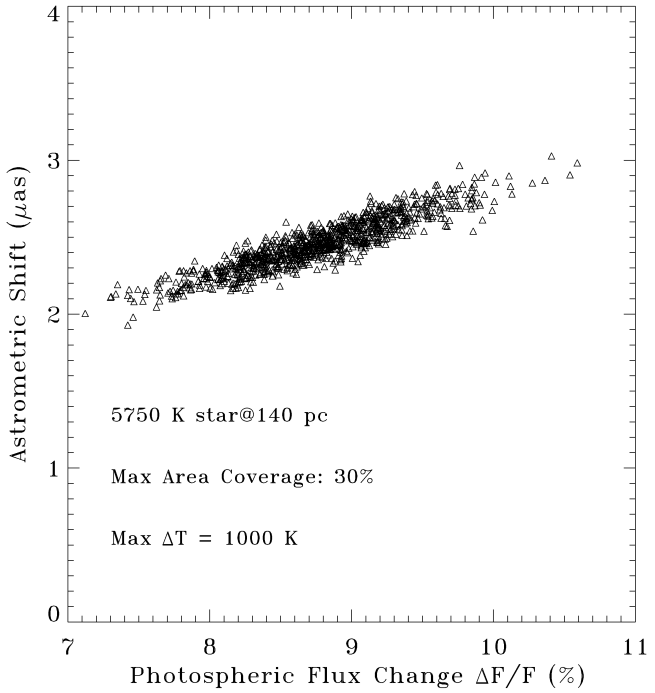

FIG. 3.—Relationship between the photometric variation $\Delta F/F$ in the visual and the photocenter shift due to starspots on a T Tauri star at 140 pc.

primarily characteristic of rapidly rotating, young stellar objects (e.g., Bouvier et al. 1995; Schuessler et al. 1996 and references therein).

In the context of a study of the effects of the variety of astrophysical sources of astrometric noise on the planet detection capabilities of *Gaia* (Sozzetti et al. 2005, in preparation), I have implemented a numerical model to calculate the photometric and astrometric effects of a distribution of spots over the surface of a rotating star. The model is based on the analytical theories developed by Dorren (1987), Eker (1994), and Eaton et al. (1996). It incorporates a broad range of spot and star parameters, including stellar limb darkening, and it allows for the presence of multiple spots of any shape, including umbra-penumbra effects.

The key result of the numerical analysis (Fig. 3) is that a photometric variation in the visual of $\Delta F/F = 10\%$ (rms) corresponds to an astrometric variation of ~ 3 μas (rms) in the position of a 1 $R_{\odot}$ pre–main-sequence (PMS) star at the distance of Taurus ($D = 140$ pc). The magnitude of the spot-induced photocenter motion on a T Tauri star is thus comparable to the gravitational effect of a Jupiter-mass object orbiting the star at 0.5 AU (~ 5 μas). The effect scales with distance, just like the astrometric signature of a planet. Thus, for a nearby, less active Sun-like star at 10 pc, its magnitude could still be of the same order (e.g., Woolf & Angel 1998), while the amplitude of the planet-induced stellar motion would be at least 1 order of magnitude larger.

However, astrometric signatures induced, for example, by a few Earth-mass planets on 1 AU orbits around solar-type stars at a distance of 10 pc and covered by spots, causing a change in photospheric flux of $\sim$1%, could be comparable in size. The nonuniformity of illumination of the stellar disk might then jeopardize successful Earth-sized planet detection with astrometry around the nearest stars, as well the detection of Jupiter-sized objects in nearby star-forming regions. Fortunately, large spotted areas on solar-type stars are relatively uncommon (the Sun itself, at its peak of activity, is covered by spots for up to $\sim$0.1% of its visible surface; see, e.g., Allen 2000). Furthermore, the spot-induced photocenter variation has a period that is strongly correlated with the photometric excursion, as well as the stellar rotation period (of an order of a few days for T Tauri stars; up to several weeks for solar-type objects). With the help of careful photometric monitoring, the two sources of astrometric signal might then be successfully disentangled.

Ultimately, in order to keep environmental and intrinsic astrophysical noise sources at the few μas level (an important cause of concern primarily for giant-planet searches in star-forming regions), it would be beneficial to avoid stars with large photometric variations, and objects with particularly large, flared disks.

3.3. Estimation Process

The estimation process applies the observable model and the noise model to the data. It includes several functions, such as search techniques, hypothesis testing, and parameter estimation. The observable model provides the estimation process with a parametric description of the expected data. The estimation process finds the observable model parameters that best match the data, with deviations weighted by the noise model. The estimation process may be a generalized least-squares method that takes advantage of the full noise covariance matrix constructed from the noise model, as I briefly describe below.

Suppose we have performed n measurements of the quantity y collected in the vector $\boldsymbol{Y}(y_1,y_2, \ldots ,y_n)$, with associated measurement uncertainties $\boldsymbol{\Sigma}(\sigma_1,\sigma_2, \ldots ,\sigma_n)$. Furthermore, call $\boldsymbol{X}(x_1,x_2, \ldots ,x_p)$ the vector of p unknown quantities that we want to determine. Let $\boldsymbol{F}(\boldsymbol{X})$ be the actual functional form of the observable model. The least-squares method will attempt to find a solution to the equation $\boldsymbol{Y} + \boldsymbol{\Sigma} = \boldsymbol{F}(\boldsymbol{X})$ in terms of the unknowns in the model.

Under the assumptions that the unknowns are normally distributed and are sufficiently small, the set of equations can be expanded to first order in the unknowns. The resulting system of "equations of condition" can be written as

$$\Delta \boldsymbol{Y} = \boldsymbol{Y} - \boldsymbol{F}(\boldsymbol{X}) = D\boldsymbol{\delta} + \boldsymbol{\Sigma}, \tag{16}$$

where $\boldsymbol{\delta}(\delta x_1, \delta x_2, \ldots, \delta x_n)$ is the vector of new unknowns, and D is the design matrix containing all partial derivatives of the observable model with respect to the unknowns. In order for the method to be applicable, the number of equations of condition must be larger than the number of unknowns, usually *at least* $n > 2p$.

The objective of the least-squares technique is to determine the vector $\boldsymbol{\delta}$ that minimizes the sum of the squares of the components of the vector of uncertainties $\boldsymbol{\Sigma}$:

$$\sum_{i=1}^{n} \sigma_i^2 = \boldsymbol{\Sigma}^T \boldsymbol{\Sigma} = (\boldsymbol{\Delta Y} - D\boldsymbol{\delta})^T (\boldsymbol{\Delta Y} - D\boldsymbol{\delta}), \tag{17}$$

where the superscript T indicates transposed. The solution is given by

$$\boldsymbol{\delta}_0 = (D^T D)^{-1} D^T \boldsymbol{\Delta Y}. \tag{18}$$

In a weighted least-squares solution, equation (16) is multiplied on both sides by a square $n \times n$ matrix G containing zeroes, except for the elements on the main diagonal, which are $g_i = \sigma_i^{-1}$. The formal solution now becomes

$$\boldsymbol{\delta}_0 = (D^T W D)^{-1} D^T W \boldsymbol{\Delta Y} = C D^T W \boldsymbol{\Delta Y}, \tag{19}$$

with the weight matrix $W = G^T G$ and the covariance matrix of the solution $C = (D^T W D)^{-1}$. The formal standard deviations of any unknown δx_i in the solution will be given by the square root of the diagonal terms of the covariance matrix c_i.

The weight matrix can be generalized in the case where correlations between the unknowns are present. In this case, nondiagonal terms will not be zero. This method is probably superior to a more conventional weighted least-squares technique, in which difference observations are formed to cancel correlated errors, and each difference is assigned a weight commensurate with the expected uncorrelated portion of the error.

The latter approach fails to take full advantage of the knowledge of the correlations, and thus residual correlated errors between successive differences persist. With a more rigorous approach, not only can one take into account any correlations that might exist, regardless of their temporal or angular scale and dependence on other observing parameters, but the correlation itself becomes part of the solution, and the self-consistency of the solution can be determined to establish to what extent the noise model is satisfactory.

If the functional form $\boldsymbol{F}(\boldsymbol{X})$ is nonlinear, as is often the case, multiple iterations of the linearized least-squares procedure must be carried out. In this case, the quality of the solution ultimately obtained (i.e., how close the minimum of the functional form adopted for the observable model is to the real one) will strongly depend on the point at which the equations are linearized. Good starting guesses of the parameters of the model would be highly desirable in order to favor the convergence of the iterative procedure. To this end, several techniques could be adopted, such as local and global minimization strategies, including the simplex method, simulated annealing, or genetic algorithms (e.g., Press et al. 1992).

Once a solution for the vector of parameters $\boldsymbol{\delta}_0$ is obtained, it is necessary to assess whether the observable model employed is indeed representative of the reality. To this end, a number of tests can be conducted.

The general procedure consists of defining a test statistic (χ^2 or its transformation $F2$, Fisher's F, and Kolmogorov-Smirnov's D) that is some function of the data measuring the distance between the hypothesis and the data, and then calculating the probability of obtaining data that have a still larger value of this test statistic than the value observed, assuming the hypothesis is true. This probability is called the confidence level. Small probabilities (say, less than 1%) indicate a poor fit. Especially high probabilities (close to 1) correspond to a fit that is too good to happen very often, and may indicate a mistake in the way the test was applied, such as treating data as independent when they are correlated.

For the purpose of planet detection, upon rejection of an observable model that assumes the star is single by means of a goodness-of-fit test, observational residuals should be inspected for the presence of hidden periodicities in the measurements. A possible approach is as follows.

First, a period search is conducted. To this end, the Lomb-Scargle periodogram analysis could be performed (e.g., Lomb 1976; Scargle 1982; Horne & Baliunas 1986). Alternatively, the observable model could be expanded to incorporate a perfectly sinusoidal term (circular orbit), and a star+circular orbit fit performed adopting a dense grid of trial periods. It should then be possible to test whether the new observable model (star+circular orbit) provides a significant improvement with respect to the single-star model. For example, a statistical test of the goodness-of-fit of the single-star and star+circular orbit model could be adopted, such as the likelihood-ratio test.

If the star+circular orbit fit performs significantly better in a measurable way, the observable model is then further expanded to include a full Keplerian orbit. In the presence of multiple planetary signals, the procedure is carried out until no further periodicities can be uncovered and the observation residuals are fully consistent with noise.

3.4. Ground-Based Experiments

The confirmation of theoretical predictions that astrometry with ground-based monopupil telescopes is limited to the mas-precision regime has been given by numerous experiments. Gatewood (1987) derived $\sigma_{\rm atm} \approx 3$ mas hr^{-1} with a reference frame of $10'$–$20'$. Han (1989) showed that a 1 mas hr^{-1} precision can be reached for a double star with $\vartheta = 1'$. Similar conclusions were derived by Gatewood (1991) and Dekany et al. (1994).

If instead of a single reference star a dense star field is used as a frame of reference, the situation improves somewhat. The theoretical predictions of $\sigma_{\rm atm} \propto A^{-1}\vartheta^{4/3}t^{-1/2}$ (Lindegren 1980) and $\sigma_{\rm atm} \propto A^{-3/2}\vartheta^{11/6}t^{-1/2}$ (Lazorenko 2002) have been substantially confirmed by Pravdo & Shaklan (1996), who demonstrated $\sigma_{\rm atm} \approx 150$ μas hr^{-1} with the 5 m Palomar Telescope using 15 reference objects in a field of 90″. These authors also showed that $\sigma_{\rm DCR} \approx 60$–$100$ μas within 1 hr of meridian crossing and at declinations within 45° of the zenith.

It is worth noting that, assuming apodization of the entrance pupil and enhanced symmetrization of the reference field, which is achieved by assigning a specific weight to each reference star, Lazorenko & Lazorenko (2004) have recently generalized the theoretical expression for the astrometric error due to the atmosphere:

$$\sigma_{\rm atm} \approx A^{-k/2+1/3}\vartheta^{k\mu/2}t^{-1/2}, \qquad (20)$$

where $2 \leq k \leq (8N_r + 1)^{1/2} - 1$, limited by the number N_r of reference objects, and $\mu \leq 1$ is a term dependent on k and the magnitude and distribution on the sky of the field stars. The classic result by Lindegren (1980) is recovered for $N_r = 1$. However, the Lazorenko & Lazorenko (2004) expression predicts $\sigma_{\rm atm} \approx 10$–$60$ μas (depending on stellar field density) for a 10 m telescope, very good seeing (FWHM = 0.″4), and $t = 600$ s. This is about a factor of 2–5 improvement with respect to the prediction of equation (15), which would have the goal of $\sigma_{\rm atm} \approx 60$ μas reached in $t = 1$ hr, for $A = 10$ m. The improvement due to this new approach to the astrometric measurement process (which, however, neglects DCR effects) still awaits experimental confirmation.

The promise of long-baseline optical/infrared interferometry for high-precision astrometry has been tested by a number of experiments in the past. The Mark-III and NPOI interferometers have achieved long-term wide-angle astrometric precision at the 10 mas level (Hummel et al. 1994). Short-term astrometric performance at the 100 μas level has been demonstrated with the Mark-III and PTI (Colavita 1994; Shao et al. 1999; Lane et al. 2000) for moderately close (30″) pairs of bright ($m_v \approx$ 2–5) stars. Recently, Lane & Muterspaugh (2004) have demonstrated that 10 μas short-term, very narrow angle astrometry is possible for a sample of close, subarcsecond binaries observed with PTI in phase-referencing mode.

The predicted astrometric performance of Keck-I (Boden et al. 1999) and VLTI (Derie et al. 2003) will presumably reach the actual limits of this technique from the ground (unless such an instrument is built at the South Pole). The two instruments have quoted limiting magnitudes in the near-infrared (2–2.4 μm) of $m_k \sim 17$–18 for narrow-angle astrometry at the 30 and 10–20 μas level, respectively, between pairs of objects separated by <20″–30″.[8]

3.5. Space-Borne Experiments

Relative, narrow-angle astrometry from space has been performed so far with the fine guidance sensors aboard *HST*, while global astrometric measurements have been carried out for the first time by *Hipparcos*.

For *HST* FGS, the data reduction of the two-dimensional interferometric measurements entails a number of ad hoc calibration and data-reduction procedures to remove a variety of random and systematic error sources from the astrometric reference frame (e.g., Taff 1990; Bradley et al. 1991; Benedict et al. 1994, 1999 and references therein). The calibration of random and systematic, long- and short-term error sources for *HST* FGS includes removing intraobservation spacecraft jitter, compensating for temperature variations and temperature-induced changes in the secondary mirror position, applying constant and time-dependent optical field angle distortion calibrations, correcting for intraorbit drift, and applying lateral color corrections during the orbit-to-orbit astrometric modeling (e.g., Benedict et al. 1994, 1999).

The global single-measurement error budget for *HST* FGS astrometry with respect to a set of reference objects near the target (within the 5″ × 5″ instantaneous field of view of FGS) had received a prelaunch estimate of ~2.7 mas by Bahcall & O'Dell (1980). Benedict et al. (1994, 1999) confirmed the overall performance level of the instrument, with single-measurement uncertainties of 1–2 mas down to $m_v = 16$. The limiting factor is the spacecraft jitter. A single-measurement precision below 0.5–1 mas is out of reach for *HST* FGS.

For *Hipparcos*, a calibration and iterative reduction procedure in five main steps (Lindegren & Kovalevsky 1989) is devised in order to derive values of positions, proper motions, and parallaxes simultaneously for ~120,000 stars by combining one-dimensional angular measurements along the satellite's instantaneous scanning direction into a global astrometric solution over the whole celestial sphere. These steps include: (1) the determination of the satellite attitude, (2) the estimation of stellar coordinates relative to the main focal grid, (3) the reference great circle (RGC) reduction, to determine the abscissae of stars on each RGC, (4) the sphere solution, to determine the correction to the great circle origins using a set of instrumental calibration parameters (including chromatic terms), and (5) the determination of the five astrometric parameters with respect to the rigid reference sphere of RGCs, using all RGC abscissae, the RGC origins, and instrumental parameters (Lindegren & Kovalevsky 1989).

[8] For astrometric planet searches conducted with these instruments, the probability of finding a reference star with $m_k = 13$ or fainter within 20″–30″ from a target object is about 50%–60%, or greater if the target is not very far from the galactic plane (Derie et al. 2003).

Typical uncertainties on the RGC abscissae are of an order of 1.0 mas for bright objects ($m_v < 7$) and degrade up to ~4.5 mas for $m_v \geq 11$ (e.g., Kovalevsky 2002).[9] These agree well with prelaunch predictions by Lindegren (1989). Without the presence of the atmosphere, and similar to *HST* FGS, the best achievable single-measurement precision is limited by the uncertainties in the determination of the along-scan attitude.

The ability to suppress systematics by at least 2 orders of magnitude for a space-borne instrument is a major technological goal. Both *SIM* and *Gaia* promise to achieve this level of astrometric precision. For the purpose of planet detection with *SIM*, in order to deliver 1 μas narrow-angle astrometry in a 1 hr integration time down to $m_v \simeq 11$–12, an accuracy on the position of the delay line of 50 pm with a 10 m baseline must be achieved (Shaklan et al. 1998). Furthermore, a positional stability for internal optical path lengths of ~10 nm is required in order to ensure maintenance of the fringe visibility (Neat et al. 1998). For a *Gaia*-like instrument, the success in meeting the goal of ≈5–10 μas single-measurement astrometric precision to hunt for planets around bright stars ($m_v < 11$–12) will depend on (1) the ability to attain CCD centroiding errors not greater than 1/1000 of a pixel in the along-scan direction (Gai et al. 2001), and (2) the capability to limit instrumental uncertainties (thermomechanical stability of telescope and focal plane assembly, and metrology errors in the monitoring of the basic angle) and calibration errors (chromaticity, satellite attitude, and focal plane–to-field coordinates transformation) down to the few μas level (e.g., Perryman et al. 2001).

4. PLANET DETECTION WITH ASTROMETRY: PAST AND PRESENT EFFORTS

Astronomers have long sought to find astrometric perturbations in a star's motion due to orbiting planet-sized companions. Many attempts have failed, some have produced more-or-less significant upper limits, and a few have been successful. I review the history of these efforts in turn.

4.1. Unfinished Tales: Barnard's Star and Lalande 21185

During the 1960s, on the basis of the analysis of over 2000 photographic plates of the Sproul Observatory covering 24 years (1938–1962), van de Kamp (1963, 1969a, 1969b) announced the discovery of perturbations in the motion of Barnard's star (GJ 699) that could be explained initially by the presence of a 1.6–1.7M_J planet on a 24–25 yr eccentric orbit, and then later in terms of two Jupiter-sized objects on coplanar, circular orbits with periods of 11.5 and 22 yr, respectively. Through the years, van de Kamp refined his results, extending the time duration of the photographic plate observations up to 43 years (1938–1981), and publishing two more papers (van de Kamp 1975, 1982). In his last interview on the subject (Schilling 1985), he still claimed that Barnard's star was orbited by two massive planets of 0.7M_J and 0.5M_J, co-revolving on circular, coplanar orbits, with periods of 12 and 20 yr, respectively.

Neither planet was ever confirmed, however. Initial claims by Jensen & Ulrych (1973) that observations were compatible with the presence of up to five planets were not verified by Gatewood & Eichhorn (1973), who could not detect any additional motion perturbing Barnard's star. The existence of giant planets orbiting the star was further cast in doubt by Hershey (1973) and Heintz (1976), who explained van de Kamp's results in terms of a number of unrecognized systematics, including telescope internal motions due to two phases of cleaning and remounting of the telescope lens 25 years after he began his observations. Years later, Fredrick & Ianna (1980), Harrington (1986), and Harrington & Harrington (1987) reported other independent studies of Barnard's star in which no wobble was detected, although van de Kamp's results were not totally discounted. Croswell (1988), on the other hand, again addressed the issue of the misinterpretation of incorrect Sproul Observatory data, concluding that unknown telescope systematics were the more likely explanation.

In a more recent study, Gatewood (1995) ruled out the presence of massive planets or brown dwarfs ($M_p > 10M_J$) around Barnard's star, while no conclusion was reached on the existence of objects of the order of the mass of Jupiter or smaller. Using *HST* FGS astrometry, Benedict et al. (1999) ruled out the presence of Jupiter-mass planets with orbital periods $P < 3$ yr, but their observations were not taken over a sufficiently long time span to address the period range of the putative planets discovered by van de Kamp. Schroeder et al. (2000) conducted a photometric study of Barnard's star and did not find any supporting evidence for the presence of massive planets and brown dwarfs at large orbital radii, in agreement with Gatewood's (1995) findings. The latest study of this star has been undertaken by Kürster et al. (2003) using precision radial velocity measurements, which allowed them to rule out the presence of planets down to the terrestrial-mass regime (a few $M_\oplus$) for objects within 1 AU. Although studies of Barnard's star have spanned more than half a century, no definitive confirmation or disproval has been established.

The possible existence of a giant planet companion (at least several Jupiter masses) to Lalande 21185 (HD 95735) was first discussed by Lippincott (1960a, 1960b) on the basis of photographic plates covering a time span of 47 years taken with the Sproul telescope. Gatewood (1974) did not find any evidence of a planetary signature at the suggested 8 yr period, but Hershey & Lippincott (1982) claimed the planetary-mass companion did exist, although on a different, longer period. Based on a limited data set covering 4 years, Gatewood et al. (1992) were not able to detect any significant perturbation in

[9] The errors on the final astrometric parameters are not only a function of m_v, but also of the ecliptic latitude β, a normal consequence of the adopted scanning law (stars at low latitudes were observed significantly less often).

the star's proper motion. However, 4 years later Gatewood (1996), in examining 50 years of radial velocity data of Lalande 21185, as well as a more sophisticated set of astrometric observations, first concluded that the star is indeed orbited by a $2.0M_J$ planet at ~10 AU, and then suggested the existence of two giant planets, the second body being less massive than Jupiter and orbiting at around 3 AU from the parent star. In this case as well, an independent confirmation has yet to be made for either of the two planets.

4.2. Upper Limits and Controversial Mass Determinations

Prompted by the success of Doppler surveys for giant planets of nearby stars and by the need to find a method to break the M_p-i degeneracy intrinsic to radial velocity measurements, several authors have in recent years reanalyzed the *Hipparcos* Intermediate Astrometric Data (IAD) in order to either detect the planet-induced stellar astrometric motion of the bright hosts, most of which had been observed by the satellite, or place upper limits to the magnitude of the perturbation, in the case of no detections. The *Hipparcos* IAD have been reprocessed alone or in combination with either the spectroscopic information or additional ground-based astrometric measurements.

The first such analysis was performed by Perryman et al. (1996), who failed to detect the astrometric motion of the first three planet-bearing stars announced: 51 Peg, 47 Uma, and 70 Vir. Based on the size of the astrometric residuals to a single-star fit, they report upper limits on companions masses in the substellar regime (7–65M_J, depending on confidence levels) for 47 UMa and 70 Vir, while limits on the companion to 51 Peg, due to its very short period, are less stringent.

Orbital fits to the *Hipparcos* IAD can be performed by using the values of P, τ, e, and ω derived from spectroscopy and by solving for a, i, and Ω, with the additional constraint (Pourbaix & Jorissen 2000):

$$\frac{a \sin i}{\pi_*} = \frac{PK\sqrt{1-e^2}}{2\pi(4.7405)}. \qquad (21)$$

With this approach, Mazeh et al. (1999) and Zucker & Mazeh (2000) published astrometric orbits for the outermost planet in the υ And system and for the planet orbiting HD 10697. The derived semimajor axes of 1.4 ± 0.6 and 2.1 ± 0.7 mas, respectively, imply companion masses of $10.1^{+4.7}_{-4.6} M_J$ and $38 \pm 13 M_J$, respectively. These values depart significantly from the minimum masses from spectroscopy, as a consequence of the small inclination angles obtained by the fitting procedures ($i = 24°$ and $10°$, respectively).

However, two subsequent studies by Gatewood et al. (2001) and Han et al. (2001) contributed to spark a controversy over the reliability of the determination of substellar companion masses with milliarcsecond astrometry. In the first work, Gatewood et al. (2001) combined the *Hipparcos* IAD with Multichannel Astrometric Photometer (MAP; Gatewood 1987) observations of ϱ CrB in an astrometric orbital solution that yielded a semimajor axis of 1.66 ± 0.35 mas, an inclination of $0\overset{\circ}{.}5$, and a derived companion mass of $0.14 \pm 0.05\ M_\odot$. The follow-up paper by Han et al. (2001) presented *Hipparcos*-based preliminary astrometric masses for 30 stars with at least one spectroscopically detected giant planet. The main conclusion of this work is that a significant fraction (~40%) of the planet candidates are instead stars, and the remaining substellar companions are in most cases brown dwarfs rather than planets. The results stem from the derivation of a vast majority of quasi–face-on orbits, with 60% of the sample having $i < 5°$ and 27% having $i < 1°$.

On the one hand, if orbits are isotropically oriented in space, the probability of finding one with $i < 1°$ is $\approx 1 \times 10^{-4}$; thus, Han et al. (2001) come to the conclusion that the sample of planet-bearing stars is severely biased toward small inclination angles. On the other hand, rather than having to reject the planet hypothesis for a substantial fraction of the Doppler candidates, the systematically very small inclination angles (and thus very large actual companion masses) could arise as an artifact of the fitting procedure. This thesis was indeed put forth by Pourbaix (2001) and Pourbaix & Arenou (2001), and later by Zucker & Mazeh (2001b). Using different statistical approaches aimed at assessing the robustness of the derived *Hipparcos* astrometric orbits, these authors demonstrated that the *Hipparcos* IAD do not have enough precision to actually reject the planet hypothesis in essentially all cases (although a few borderline cases do exist). Thus, essentially all the preliminary astrometric masses derived for stars with planets observed with *Hipparcos* (Mazeh et al. 1999; Zucker & Mazeh 2000; Gatewood et al. 2001; Han et al. 2001) do not survive close statistical scrutiny.

The *Hipparcos* IAD can still be used, however, to set upper limits on the size of the astrometric perturbations, as done by Perryman et al. (1996) and by Zucker & Mazeh (2001b), who could rule out at the ~2 σ level the hypothesis of low-mass stellar companions disguised as planets for over two dozen objects. This, combined with the fact that the same analysis of *Hipparcos* data reveals instead that a significant fraction of the proposed brown dwarf companions from spectroscopy are stellar in nature, is interpreted as further evidence of the existence of the brown dwarf desert that separates stellar- and planetary-mass secondaries.

In the end, the only *firm* upper limits on the mass of a spectroscopically detected extrasolar planet are those placed by McGrath et al. (2002, 2004), who failed to reveal astrometric motion of the $M_p \sin i = 0.88 M_J$ object on a 14.65 day orbit in the ϱ^1 Cnc multiple-planet system using *HST* FGS astrometry. With a nominal single-measurement precision of 0.5 mas, the failed attempt at detecting any reflex motion in the data implies that the 1.15 mas preliminary *Hipparcos*-based mass

estimate by Han et al. (2001) is ruled out at the 3–5 σ level, thus establishing an updated mass upper limit of $\sim 30 M_J$ and firmly confirming that the object is substellar in nature.

4.3. Actual Measurements and Work in Progress

It was not until 2 years after the first confirmation of the planetary nature of the companion to HD 209458 via detection of its transits across the disk of the parent star (Charbonneau et al. 2000; Henry et al. 2000) that astrometric techniques finally provided the first undisputed value of the actual mass of a Doppler-detected planet. Narrow-field relative astrometry of the multiple-planet host star GJ 876 was carried out by Benedict et al. (2002) using *HST* FGS.

The goal of this project was to determine the astrometric wobble induced on the parent star by the outer planet. At a distance $D = 4.7$ pc, and with a nominal primary mass of the M4 dwarf star $M_* = 0.32\ M_\odot$, the planet with a projected mass $M_p \sin i \sim 2 M_J$ on a $P = 60$ day orbit was predicted to produce a minimum gravitational perturbation of $\sim 270\ \mu$as, which was deemed detectable by the typical 0.5 mas single-measurement precision of *HST* FGS. Benedict et al. (2002) used five reference stars within a few arcminutes from the target and derived the perturbation size, inclination angle, and mass of GJ 876b from a combined fit to the available astrometry and spectroscopy. They found $\alpha = 250 \pm 60\ \mu$as, $i = 84° \pm 6°$, and $M_p = 1.89 \pm 0.34 M_J$.

In the recent announcement (McArthur et al. 2004) of the discovery of a Neptune-sized planet on a 2.8 day orbit in the ϱ^1 Cnc system (which brought the number of planets in the system to a total of four), *HST* FGS astrometry again played an important role. The authors in fact reanalyzed the available data on ϱ^1 Cnc that had allowed McGrath et al. (2002, 2004) to put stringent upper limits on the mass of the 14.65 day period planet, and estimated, from the small arc of the orbit covered in the limited *HST* data set, a perturbation size (1.94 ± 0.4 mas) and inclination ($53° \pm 6\overset{\circ}{.}8$) for the outermost planet, orbiting at ~ 5.9 AU. Under the assumption of perfect coplanarity of all planets in the system, this implies an actual mass of $17.7 \pm 5.57\ M_\oplus$ for the innermost planet.

Currently, Benedict et al. (2003a, 2003b, 2004) are monitoring the stars υ And and ε Eri with *HST* FGS and plan to combine the data with the available radial velocity data sets and with lower per-measurement precision ground-based astrometry. The predicted minimum perturbation sizes of the long-period (3.51 and 6.85 yr, respectively) planets orbiting these stars ($\alpha_{\upsilon\ \mathrm{And}} \simeq 540\ \mu$as and $\alpha_{\varepsilon\ \mathrm{Eri}} \simeq 1120\ \mu$as, respectively) should be clearly detectable with *HST* FGS, given a sufficient time baseline for the observations.

5. FUTURE PROSPECTS

A number of authors have tackled the problem of evaluating the sensitivity of the astrometric technique required to detect extrasolar planets and reliably measure their orbital elements and masses. In particular, the works by Casertano et al. (1996), Lattanzi et al. (1997, 2000a, 2000b, 2002, 2005), and Sozzetti et al. (2000, 2001, 2003b) were specifically tailored to *Gaia*; those of Casertano & Sozzetti (1999), Sozzetti et al. (2002, 2003a), Ford & Tremaine (2003), Ford (2004), and Marcy et al. (2005) were instead centered on *SIM*. Black & Scargle (1982) and Eisner & Kulkarni (2001, 2002) studied the general problem of the detectability of periodic signals with the astrometric technique alone or in combination with spectroscopic measurements, while Konacki et al. (2002) and Pourbaix (2002) explored to some extent the reliability of orbit reconstruction of future astrometric missions when all parameters have to be derived from scratch, in the limit of high and low S/Ns.

The abovementioned exploratory works, which provided a first assessment of the planet detection capabilities of *Gaia* and *SIM*, adopted a qualitatively correct description of the measurements each mission will carry out. For *Gaia*, the then-current scanning law was adopted, while for *SIM*, reference stars and realistic observation overheads were included. The authors implemented realistic data analysis techniques based on both the χ^2 test and periodogram search for estimating detection probabilities as well as nonlinear least-squares fits to the data to determine orbital parameters and planet masses ranging from $1 M_J$ down to $1\ M_\oplus$.

From the point of view of data simulation, the major simplifying assumption of these studies is the idealization of the adopted instrument. Measurement errors assume simple Gaussian distributions, and knowledge of the spacecraft attitude is assumed to be perfect, with no additional instrumental effects, measurement biases, or calibration imperfections. In terms of data analysis procedures, the most relevant simplification is the adoption of perturbations of the true values of all parameters as initial guesses for the nonlinear fits, largely neglecting the difficult problem of identifying from scratch adequate configurations of starting values.

5.1. Planet Detection

Detection probabilities are determined based on a χ^2 test of the null hypothesis that there is no planet. Five-parameter, single-star fits to the simulated data sets are carried out, and observation residuals are inspected. Residuals that are large compared to the assumed single-measurement precision will induce a failure of the χ^2 test at a given confidence level.

The two parameters upon which detection probabilities mostly depend are the astrometric signal-to-noise ratio α/σ_m and the period P, while eccentricity and orientation in the plane of the sky do not significantly affect planet detectability. Figure 4 shows isoprobability contours for *SIM* as a function of α/σ_m and P, based on a χ^2 test with a confidence level of 95%.

For both instruments, assuming a realistic number of data points throughout the nominal mission lifetimes $T = 5$ yr,

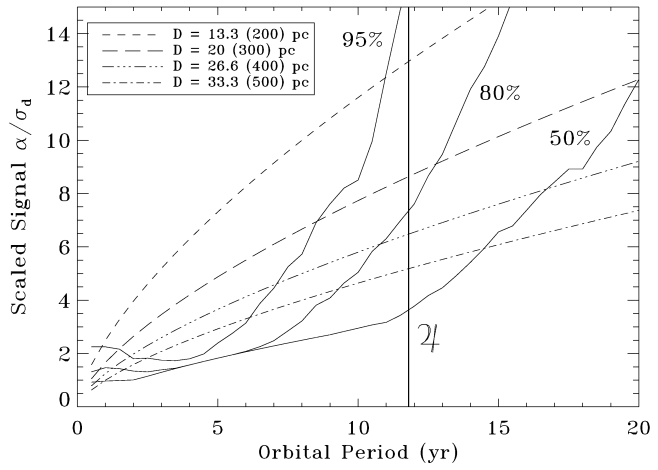

FIG. 4.—Isoprobability contours for planet detection with *SIM* at the 95% confidence level. The results are expressed as a function of P and α/σ_m and averaged over all orbital parameters. The dashed lines indicate the equivalent signature at the given distance for a system composed of a solar-mass primary and a 20 $M_\oplus$ planet ($1M_J$ in parentheses). (Reprinted with permission from Sozzetti et al. 2002.)

$\alpha/\sigma_m \simeq 2$ is sufficient to detect planetary signatures for $P \leq T$. As orbital sampling gets increasingly worse for $P > T$, the required signal rises sharply, especially for high detection probabilities. The same qualitative behavior of generic detection curves was recovered by Eisner & Kulkarni (2001), who also provided analytical expressions for the behavior of the astrometric sensitivity to planetary signatures in the two regimes.

5.2. Orbit Reconstruction and Mass Determination

Upon detection of its signal, the goal of determining a planet's orbital characteristics and mass requires the adoption of observable models with at least 12 parameters (5 astrometric plus 7 describing the full Keplerian motion). For *SIM*, the model is further complicated by the simultaneous solution for the astrometric parameters of the local frame of reference (5 for each astrometrically clean reference star). The simultaneous fit to both astrometric and orbital parameters strongly reduces the covariance between proper motion and astrometric signature pointed out by Black & Scargle (1982), in particular for $P \leq T$.

A standard metric used to understand how well the observable model performs on the simulated data is the convergence probability; i.e., the fraction of the final values of each parameter that falls within a given fractional error of the true values. I show in Figure 5 the *Gaia* convergence probability to 10% fractional uncertainty for a, P, e, and i as a function of the distance from the Sun for a Jupiter-Sun system with $P \ll T$, $P \simeq T$, and $P \gg T$.

As a general result, $\alpha/\sigma_m \simeq 5$ is required for orbit reconstruction and mass determination at the 20%–30% accuracy level, while $\alpha/\sigma_m \simeq 10$–$15$ is necessary for a more stringent 10% accuracy requirement.

As can be seen in Figure 5, orbital periods that are twice as long as the mission duration induce significant degradation in the quality of the orbit reconstruction, although different parameters are affected differently. For example, the correct period of the signal is more easily identified, as it is independent of the Keplerian nature of the problem (e.g., Monet 1979). Short periods also cause a degradation of the results, due to the increasingly smaller amplitude of the perturbation, an effect that overruns the increasingly larger number of orbital revolutions sampled during the mission duration.

Orbital eccentricity also plays a very significant role when attempting to obtain an orbital solution. The deterioration of orbit determination is especially prominent for long-period planets, for which the limited orbital sampling couples with large values of e, with the result that orbits are increasingly more unlikely to be sampled during pericenter passage, and the correct orbit size and geometry become very difficult to identify correctly.

On the other hand, the inclination of the orbital plane does not very significantly impact the ability to accurately determine the orbital parameters and mass of a planet, unless $i \rightarrow 90°$. In quasi–edge-on configurations, in fact, the projected stellar motion is reduced to one dimension, and a considerable amount of information is lost. However, this effect is already negligible for configurations departing from exactly edge-on by a few degrees (Eisner & Kulkarni 2002; Ford 2004).

Finally, unlike *Gaia*, *SIM* will have the leisure to choose the number N_o and timing of the observations, as well as the number N_r of reference objects. Both the detection probabilities and the quality of orbit determination are sensitive to these parameters, with simple parameterizations given by $\sim\sqrt{N_o}$ and $\sim\sqrt{N_r}$ (Sozzetti et al. 2002). Ford (2004) has studied in detail a wide range of possible observing schedules, and concluded that both planet detection and orbit reconstruction are relatively insensitive to the specific choice of the distribution of observations.

5.3. Multiple-Planet Systems

The limiting ability to detect and characterize planetary systems with μas astrometry has been estimated by Sozzetti et al. (2001, 2003a), using as test cases the then-current lists of multiple-planet systems discovered by Doppler surveys. In their works, the authors neglected any complications stemming from significant perturbations of the planetary orbits due to strong planet-planet secular or resonant dynamical interactions.

Under the assumption of sufficient data redundancy with respect to the number of parameters in the observable model

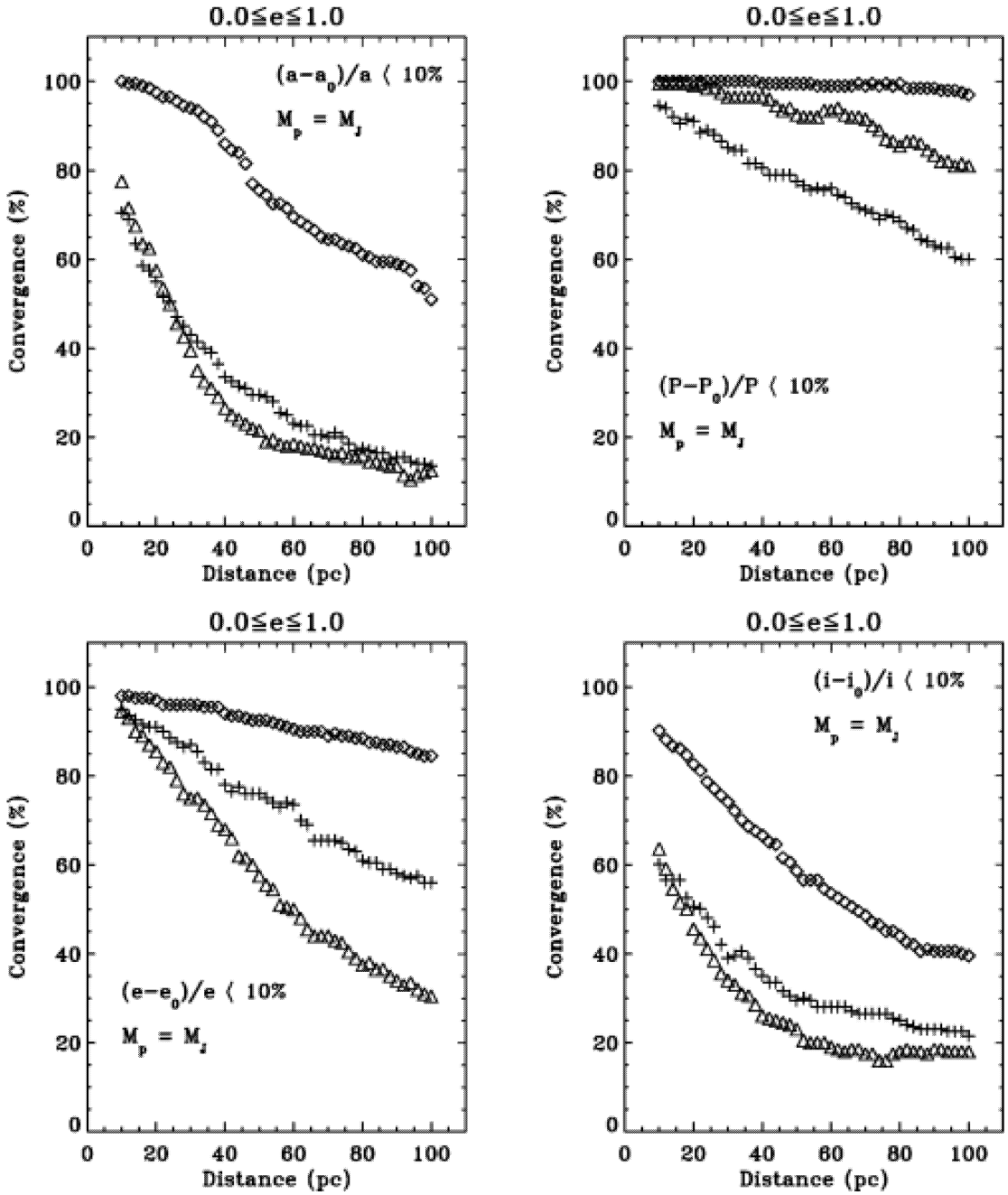

FIG. 5.—*Gaia* convergence probability to a 10% accuracy for *a*, *P*, *e*, and *i*, as a function of the distance from the Sun. A Sun-Jupiter system is assumed. Symbols of different shapes correspond to different periods: triangles for 0.5 yr, diamonds for 5 yr, and crosses for 11.8 yr. (Reprinted with permission from Lattanzi et al. 2000b.)

fitted to the observation,[10] the detection of additional components in a system can be reliably carried out. Only borderline cases, in which a signal with $\alpha/\sigma_m \simeq 1$ is not properly modeled and subtracted, will produce a significant increase in the false detection rates. For such cases, and in the limit for $P \leq T$, a period search would add robustness to the detection method, while the least-squares technique combined with Fourier anal-

[10] If $N_{\rm pl}$ is the number of planets in the system, then *at least* $N_o > 2(5 + 7N_{\rm pl})$ for *Gaia*, and $N_o > 2(5 + 7N_{\rm pl} + 5N_r)$ for *SIM*, is required.

ysis would arguably be preferred when attempting to detect signals with $P > T$.

The typical accuracy of multiple-planet orbit reconstruction and mass determination would be degraded by 30%–40% with respect to the single-planet case, a relatively modest deterioration, particularly for well-sampled, well-spaced orbits with $\alpha/\sigma_m \geq 10$.

The ability of astrometry to determine the full set of orbital parameters implies that for favorable multiple-planet configurations it should be possible to derive a meaningful estimate of the relative inclination angle (e.g., Kells et al. 1942):

$$\cos i_{\rm rel} = \cos i_{\rm in} \cos i_{\rm out} + \sin i_{\rm in} \sin i_{\rm out} \cos (\Omega_{\rm out} - \Omega_{\rm in}), \quad (22)$$

where ($i_{\rm in}$, $i_{\rm out}$) and ($\Omega_{\rm in}$, $\Omega_{\rm out}$) are the inclinations and lines of nodes of the inner and outer planet, respectively.

I show in Figure 6 the estimated accuracy with which *SIM* could determine the coplanarity (i.e., $i_{\rm rel} \simeq 0.0$) between pairs of planetary orbits as a function of the common inclination angle for 11 known multiple-planet systems.

For configurations in which all components produce $\alpha/\sigma_m \gtrsim 10$, coplanarity could be established, with typical uncertainties of a few degrees, for periods up to twice the mission duration. In systems where at least one component has $\alpha/\sigma_m \rightarrow 1$, accurate coplanarity measurements are compromised, and mutual inclinations can only be determined with uncertainties of several tens of degrees.

Finally, if combined radial velocity+astrometric solutions were to be carried out on single- or multiple-planet systems, the quality of orbit reconstruction and mass determination would be significantly improved, especially in the long-period regime ($P > T$) and for edge-on configurations, while well-sampled, well-measured orbits ($P \leq T$, $\alpha/\sigma_m \gg 1$) would be only marginally improved by radial velocity+astrometric solutions (Eisner & Kulkarni 2002; Sozzetti et al. 2003a, 2003b).

5.4. The Search for Good Starting Values

The convergence of nonlinear fitting procedures and the quality of orbital solutions can both be significantly affected by the choice of the starting guesses. In the absence of any kind of a priori information on the actual presence of planets around a given target, all orbital parameters will have to be derived from scratch. The results of, e.g., Han et al. (2001) already provided a word of caution on the reliability of low-S/N astrometric orbits, even when constraints on some of the parameters are available from spectroscopy. It is thus crucial to investigate new strategies in the fitting procedure to maximize the robustness of the solutions obtained.

Pourbaix (2002) tackled the problem in the context of work on the precision achievable in the orbital parameters of astrometric binaries from two- and one-dimensional observations, in the case of low S/N. He proposed a two-dimensional global grid search approach in the (e, τ) space, coupled with a guess on P by means of a period search technique (e.g., Horne & Baliunas 1986) while fitting a linearized model in the four Thiele-Innes elements (e.g., Green 1985).

Konacki et al. (2002) applied a "frequency decomposition" method to simulated *SIM* observations of υ And. This approach is based on a Fourier expansion of the Keplerian motion, in which the coefficients of the successive harmonics are functions of all orbital elements. The values of the latter, obtained from the linear least-squares solution performed with the Fourier expansion, are then used as starting guesses of a local minimization of the nonlinear problem. This method avoids the complications of a global-search approach in several dimensions, which can be very computationally intensive. However, the authors did not attempt to validate their approach in cases departing from the favorable ($P \leq T$, $\alpha/\sigma_m \gg 1$) configuration studied.

The most detailed study on this subject is the one currently being carried out by the *Gaia* Planetary Systems Working Group. Lattanzi et al. (2005) have recently presented preliminary results of an ongoing, large-scale double-blind test campaign that has been set up in order to provide a realistic assessment of the *Gaia* capabilities in detecting extrasolar planets.

The double-blind test protocol envisions three distinct groups of participants. The "simulators" define and generate simulated observations of stars with and without planets with a *Gaia*-like satellite; the "solvers" define detection tests, with levels of statistical significance of their own choice, and orbital fitting algorithms, using any local, global, or hybrid solution method that they determine is best; and the "evaluators" compare simulations and solutions and draw a first set of conclusions on the process.

As an illustrative example, Figure 7 shows one of the results of a simulation of 50,000 stars orbited by a single planet having $0.2 \leq P \leq 12$ yr and producing $2 \lesssim \alpha/\sigma_m \lesssim 100$. The current *Gaia* scanning law is used, with a single-measurement precision $\sigma_m = 8$ μas. The plot shows how the periods derived by one of the solvers compare to the true simulated ones. The most striking result is the ability to derive very accurate estimates of the period for $P \leq 6$ yr for the full range of α/σ_m and for all possible values of $0 \leq e \leq 1$ and $0° \leq i \leq 90°$. For periods exceeding the mission duration by over 20%, it becomes increasingly difficult to identify the correct value of P. In this case, part of the signal can be absorbed in the stellar proper motion, with the net result that the size and period of the perturbation are systematically underestimated.

However, the preliminary findings by Lattanzi et al. (2005) show that "mission-ready" detection and orbital fit packages (including reliable estimates of the covariance matrix of the solutions) tailored to future high-precision astrometric observatories, requiring no a priori knowledge of the orbital elements, can already achieve good levels of performance.

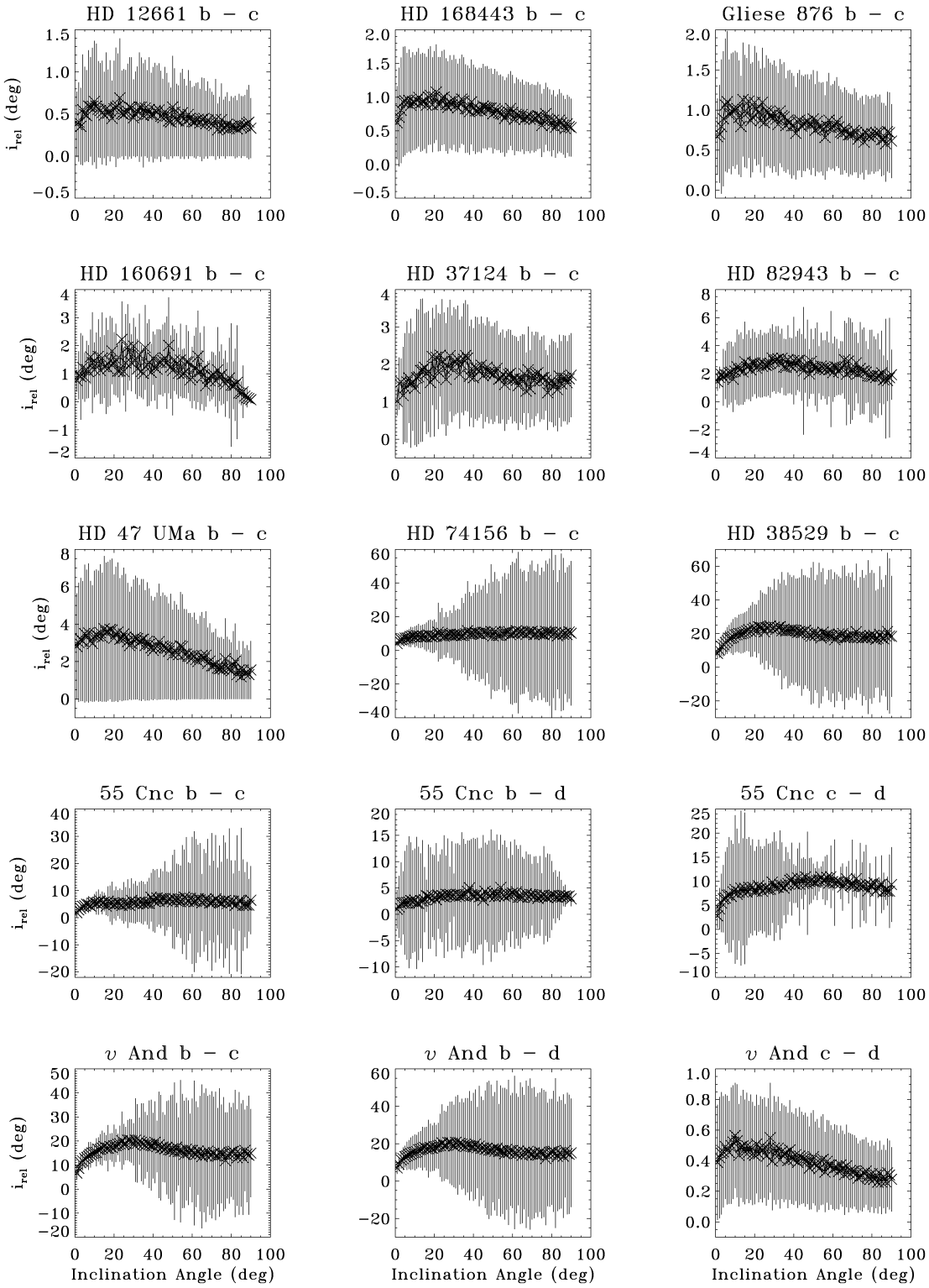

FIG. 6.—Mutual inclination i_{rel} between pairs of planetary orbits, as a function of the common inclination angle with respect to the line of sight, for 11 multiple-planet systems measured by *SIM*. In each panel, the corresponding uncertainties are computed using the formal expressions from the covariance matrix of the multiple Keplerian fit. (Reprinted with permission from Sozzetti et al. 2003a.)

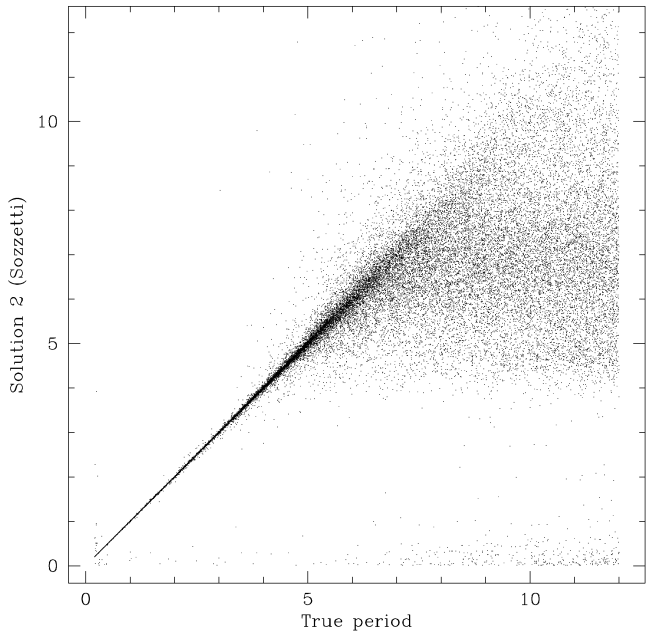

FIG. 7.—True vs. derived orbital periods (in yr) for a set of 50,000 orbital solutions in the context of the double-blind test campaign for planet detection with *Gaia*.

6. DISCUSSION: ASTROMETRY IN PERSPECTIVE

The classic way to gauge the effectiveness of different planet search techniques is to compare their respective discovery spaces, defined in terms of the planets of given mass and period that each method will be able to detect. As an illustrative example, Figure 8 shows an M_p-P diagram that plots current sensitivities of transit photometry and radial velocity, as well as the expected *SIM* and *Gaia* detection thresholds at 10 and 150 pc, respectively. For the radial velocity detection curve, the simulations by Sozzetti et al. (2005) were used, while for *SIM* and *Gaia*, the Sozzetti et al. (2002, 2003b) results were used. The sensitivity for transit photometry was derived based on the Gaudi et al. (2005) analytical dependence of the detectable planet radius R_p on $P^{1/6}$ (converted to $M_p \propto P^{1/2}$, assuming constant planet density), under the (naive) hypothesis of uniform sampling.

Simply taking at face value the curves of Figure 8, however, can lead to important misunderstandings about the intrinsic relevance of the different techniques to planetary science. For example, the sensitivity of photometric techniques to transiting planets with $P \gtrsim 10$ days is strongly suppressed, and this detection method is useless if the planet does not transit. However, the information this technique provides for the very close-in objects discovered is extremely valuable, and it cannot be provided by radial velocity and astrometry.

A more effective way to proceed is thus to gauge the relative importance of different planet detection techniques by looking at their discovery potential not per se, but rather in connection to outstanding questions to be addressed and answered in the science of planetary systems, such as those listed at the end of § 2. I summarize below some of the most important issues for which μas astrometry will play a key role.

6.1. The Hunt for Other Earths

The holy grail in extrasolar planet science is clearly the direct detection and characterization of Earth-sized, habitable planets with atmospheres where biomarkers (e.g., Lovelock 1965; Ford et al. 2001b; Des Marais et al. 2002; Selsis et al. 2002; Seager & Ford 2005) might be found that could give clues to the possible presence of life forms. Imaging terrestrial planets is currently the primarily science goal of the coronagraphic and interferometric configurations of the *Terrestrial Planet Finder* (*TPF*; Beichman et al. 2002) and of the *Darwin* mission (Fridlund 2000).

Space-borne transit photometry carried out with *COROT* (Baglin et al. 2002) or *Kepler* (Borucki et al. 2003) has the potential to be the first technique to make such a detection. However, astrometry of all nearby stars within 10–20 pc of the Sun at the μas level (with *SIM* and *Gaia* in space, and possibly with Keck-I and VLTI from the ground) will be an essential ingredient in providing *Darwin*/*TPF* with (1) systems containing bona fide terrestrial, habitable planets (Ford & Tremaine 2003; Sozzetti et al. 2002; Marcy et al. 2005), and (2) a comprehensive database of F-G-K-M stars with and without detected giant planets orbiting out to a few AU from which to choose additional targets based on the presence or absence of Jupiter signposts (Sozzetti et al. 2003b). Such measurements will uniquely complement ongoing and planned radial velocity programs aiming at $\lesssim 1$ m s^{-1} precision (e.g., Santos et al. 2004b), and exozodiacal dust emission observations from the ground with Keck-I, LBTI, and VLTI.

6.2. Statistical Properties and Correlations

As discussed in §§ 2.1 and 2.2, planet properties (orbital elements and mass distributions, and correlations among them) and frequencies are likely to depend on the characteristics of the parent stars (spectral type, age, metallicity, and binarity/multiplicity). It is thus desirable to be able to provide as large a database as possible of stars screened for planets.

The size of the stellar sample screened for planets by an all-sky astrometric survey such as *Gaia* (Lattanzi et al. 2000b) could be on the order of a few hundred thousand relatively bright ($m_v < 13$) stars, with a wide range of spectral types, metallicities, and ages out to ~150 pc. The sample size is thus comparable to that of planned space-borne transit surveys, such as *COROT* and *Kepler*. The statistical value of such a sample is better understood when one considers that depending on actual giant planet frequencies as a function of spectral type

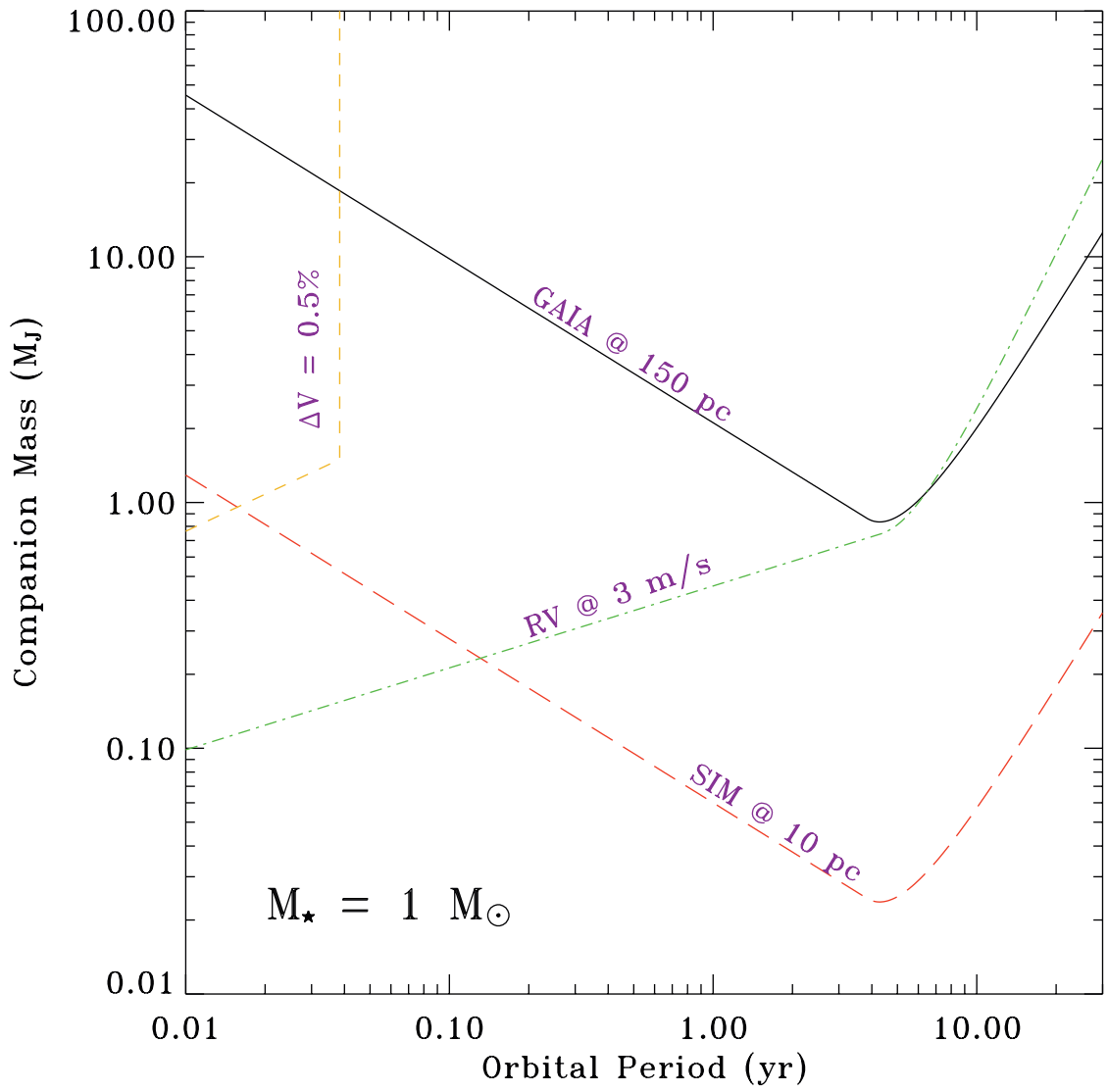

FIG. 8.—Planet discovery space in the M_p-P diagram for different techniques. Detection curves are defined on the basis of a 3 σ criterion. For *SIM* and *Gaia*, $\sigma_m = 2$ and 8 μas are assumed, respectively. For radial velocities, $\sigma_m = 3$ m s^{-1}. Finally, for transit photometry, $\sigma_m = 5$ mmag. The time span of the observations is set to $T = 5$ yr.

and orbital distance, at least a few thousand planets could be detected and measured (Lattanzi et al. 2002). This number is comparable to the current size of the target lists of ground-based Doppler surveys. Finally, the ranges of orbital parameters and planet host characteristics probed by an all-sky astrometric planet survey would crucially complement both transit observations (which strongly favor short orbital periods and are subject to stringent requisites on favorable orbital alignment) and radial velocity measurements (which can be less effectively carried out for stars covering a wide range of spectral types, metallicities, and ages and do not allow for the determination of either the true planet mass or the full three-dimensional orbital geometry).

6.3. Tests of Giant Planet Formation and Migration

The competing giant planet formation models make very different predictions regarding formation timescales, planet mass ranges, and planet frequency as a function of host star characteristics. Furthermore, correlations between orbital elements and masses, and possibly between the former and some of the host star characteristics (metallicity), might reflect the

outcome of a variety of migration processes and their possible dependence on environment (see §§ 2.1 and 2.2). These predictions could be tested on firm statistical grounds by extending planet surveys to large samples of PMS objects and field metal-poor stars.

The full sample of ~1500 relatively bright ($m_v < 13$), nearby ($D \lesssim 150$–200 pc), field metal-poor stars currently known could be screened for giant planets on wide orbits by *Gaia* or *SIM*, thus complementing the shorter period ground-based spectroscopic surveys (Sozzetti et al. 2005), which are also limited in sample size, due to the intrinsic faintness and weakness of the spectral lines of the targets. Combined, these data would allow for an improved understanding of the behavior of the probability of planet formation in the low-metallicity regime, by direct comparison between large samples of metal-poor and metal-rich stars, in turn putting stringent constraints on the proposed planet formation models. Disproving or confirming the existence of the *P*-[Fe/H] correlation would also help us to understand whether metallicity plays a significant role in the migration scenarios for giant planets.

High-precision astrometric measurements of at least a few hundred relatively bright ($m_v < 13$–14) PMS stars in a dozen nearby ($D < 200$ pc) star-forming regions could be carried out with *SIM* and *Gaia*, searching for planets orbiting at 1–5 AU. The possibility of determining the epoch of giant planet formation in the protoplanetary disk would provide the definitive observational test to distinguish between the proposed theoretical models. These data would uniquely complement near- and mid-infrared imaging surveys (e.g., Burrows 2005 and references therein) for direct detection of young, bright, wide-separation ($a > 30$–100 AU) giant planets.

6.4. Dynamical Interactions in Multiple-Planet Systems

The different sources of dynamical interactions proposed to explain the highly eccentric orbits of planetary systems (see § 2.1) give rise to significantly different orbital alignments. An effective way to understand their relative roles would involve measuring the relative inclination angle between pairs of planetary orbits. Studies addressing the long-term dynamical stability of multiple-planet systems, as well as the possibility of formation and survival of terrestrial planets in the habitable zone of the parent star (see § 2.3), would also greatly benefit from knowledge of whether pairs of planetary orbits are coplanar or not.

The only way to provide meaningful estimates of the full three-dimensional geometry of *any* planetary system (without restrictions on the orbital alignment with respect to the line of sight) is through direct estimates of the mutual inclinations angles using high-precision astrometry (Sozzetti et al. 2001, 2003a). For a *Gaia*-like all-sky survey instrument, the database of potential targets out to 50–60 pc is of the order of a few tens of thousands of objects (Sozzetti et al. 2001). These data, combined with those available from Doppler measurements and transit photometry and timing (e.g., Miralda-Escudé 2002; Holman & Murray 2005; Agol et al. 2005), would then allow us to put studies of the dynamical evolution of planetary systems on firmer ground.

6.5. Concluding Remarks

Despite several decades of attempts, and a few recent successes, astrometric measurements with milliarcsecond precision have so far proved of limited utility as a tool to search for planetary-mass companions orbiting nearby stars. However, an improvement of 2–3 orders of magnitude in achievable measurement precision, down to the few μas level, would allow this technique to achieve in perspective the same successes as the Doppler method, for which the improvement from the km s^{-1} to the few m s^{-1} precision opened the doors for groundbreaking results in planetary science.

In this paper I have reviewed a series of technological, statistical, and astrophysical issues that future ground-based and space-borne efforts will have to face in their attempts to discover planets. At the μas precision level, independent of the type of instrument used (either filled- or diluted-aperture telescopes), a number of important modifications to the standard definition of astrometric observable (the stellar position in the instrument-specific reference frame) will have to be introduced, such as subtle effects due to general relativity. Astrophysical noise sources that may mimic the presence of a planet, such as significant stellar surface activity, will have to be taken into account. Several tools will have to be considered when attempting to derive reliable orbital solutions, such as optimized strategies to find good initial configurations for the orbital parameters. However, the greatest challenge will be to build instrumentation, both on the ground (Keck-I, VLTI) and in space (*SIM* and *Gaia*), that is capable of attaining the technologically demanding requirements needed to achieve a targeted single-measurement precision $\sigma_m \simeq 1$–10 μas. Provided that these are met, astrometry during the next decade has the potential to provide critical contributions to planetary science, which are crucially needed in order to complement the expectations from other indirect and direct planet detection methods, and to refine theoretical understanding, for continuous improvements in the field of the formation and evolution of planetary systems.

During the preparation of this manuscript, I have benefited from very fruitful discussion with many colleagues. I am particularly grateful to A. P. Boss, S. Casertano, D. Charbonneau, D. W. Latham, M. G. Lattanzi, G. W. Marcy, M. Mayor, D. Pourbaix, D. Queloz, D. D. Sasselov, and G. Torres for helpful comments and insights. I thank an anonymous referee for a very critical revision of an earlier version of this paper, and for illuminating suggestions and recommendations that greatly improved the manuscript. The author acknowledges support from the Smithsonian Astrophysical Observatory through the SAO Predoctoral Fellowship program and the Keck

PI Data Analysis Fund (JPL 1262605). This research has made use of NASA's Astrophysics Data System Abstract Service and of the SIMBAD database, operated at CDS, Strasbourg, France.

REFERENCES

Agol, E., Steffen, J., Sari, R., & Clarkson, W. 2005, MNRAS, 359, 567
Alibert, Y., Mordasini, C., & Benz, W. 2004, A&A, 417, L25
Alibert, Y., Mordasini, C., Benz, W., & Winisdoerffer, C. 2005, A&A, 434, 343
Allen, C. W. 2000, Allen's Astrophysical Quantities (4th ed.; New York: Springer)
Alonso, R., et al. 2004, ApJ, 613, L153
Armitage, P. J., Livio, M., Lubow, S. H., & Pringle, J. E. 2002, MNRAS, 334, 248
Armstrong, J. T., et al. 1998, ApJ, 496, 550
Baglin, A., et al. 2002, in ASP Conf. Ser. 259, Radial and Nonradial Pulsations as Probes of Stellar Physics, ed. C. Aerts, T. R. Bedding, & J. Christensen-Dalsgaard (San Francisco: ASP), 626
Bahcall, J. N., & O'Dell, C. R. 1980, in Proc. IAU Colloq. 54, Scientific Research with the Space Telescope, ed. M. S. Longair & J. W. Warner (NASA CP-2111; Washington: NASA), 5
Baraffe, I., Selsis, F., Chabrier, G., Barman, T. S., Allard, F., Hauschildt, P. H., & Lammer, H. 2004, A&A, 419, L13
Barnes, R., & Quinn, T. 2004, ApJ, 611, 494
Barnes, R., & Raymond, S. N. 2004, ApJ, 617, 569
Beer, M. E., King, A. R., Livio, M., & Pringle, J. E. 2004, MNRAS, 354, 763
Beichman, C. A., Coulter, D. R., Lindensmith, C., & Lawson, P. R. 2002, Proc. SPIE, 4835, 115
Belokurov, V. A., & Evans, N. W. 2002, MNRAS, 331, 649
Benedict, G. F., et al. 1994, PASP, 106, 327
———. 1999, AJ, 118, 1086
———. 2002, ApJ, 581, L115
———. 2003a, BAAS, 35, 07.10
———. 2003b, BAAS, 35, 67.05
———. 2004, BAAS, 36, 42.02
Black, D. C., & Scargle, J. D. 1982, ApJ, 263, 854
Boden, A. F., Colavita, M. M., Lane, B. F., Shao, M., van Belle, G. T., & Lawson, P. R. 1999, in ASP Conf. Ser. 194, Working on the Fringe: Optical and IR Interferometry from Ground and Space, ed. S. Unwin & R. Stachnik (San Francisco: ASP), 84
Bodenheimer, P., Laughlin, G., & Lin, D. N. C. 2003, ApJ, 592, 555
Bodenheimer, P., Lin, D. N. C., & Mardling, R. A. 2001, ApJ, 548, 466
Borucki, W. J., et al. 2003, Proc. SPIE, 4854, 129
Boss, A. P. 1997, Science, 276, 1836
———. 1998, Nature, 393, 141
———. 2000, ApJ, 536, L101
———. 2001, ApJ, 563, 367
———. 2002, ApJ, 567, L149
———. 2004, ApJ, 610, 456
Bouchy, F., Pont, F., Santos, N. C., Melo, C., Mayor, M., Queloz, D., & Udry, S. 2004, A&A, 421, L13
Bouvier, J., Covino, E., Kovo, O., Martin, E. L., Matthews, J. M., Terranegra, L., & Beck, S. C. 1995, A&A, 299, 89
Bradley, A., Abramowicz-Reed, L., Story, D., Benedict, G., & Jefferys, W. 1991, PASP, 103, 317
Brown, T. M., Charbonneau, D., Gilliland, R. L., Noyes, R. W., & Burrows, A. 2001, ApJ, 552, 699
Brumberg, V. A. 1991, Essential Relativistic Celestial Mechanics (Bristol: Hilger)
Burrows, A. 2005, Nature, 433, 261
Burrows, A., Hubeny, I., & Sudarsky, D. 2005, ApJ, 625, L135
Butler, R. P., Vogt, S. S., Marcy, G. W., Fischer, D. A., Wright, J. T., Henry, G. W., Laughlin, G., & Lissauer, J. J. 2004, ApJ, 617, 580
Casertano, S., Lattanzi, M. G., Perryman, M. A. C., & Spagna, A. 1996, Ap&SS, 241, 89
Casertano, S., & Sozzetti, A. 1999, in ASP Conf. Ser. 194, Working on the Fringe: Optical and IR Interferometry from Ground and Space, ed. S. Unwin & R. Stachnik (San Francisco: ASP), 171
Charbonneau, D., Brown, T. M., Latham, D. W., & Mayor, M. 2000, ApJ, 529, L45
Charbonneau, D., Brown, T. M., Noyes, R. W., & Gilliland, R. L. 2002, ApJ, 568, 377
Charbonneau, D., et al. 2005, ApJ, 626, 523
Colavita, M. M. 1994, A&A, 283, 1027
———. 1999, PASP, 111, 111
Colavita, M. M., et al. 1999, ApJ, 510, 505
Correia, A. C. M., Udry, S., Mayor, M., Laskar, J., Naef, D., Pepe, F., Queloz, D., & Santos, N. C. 2005, A&A, 440, 751
Croswell, K. 1988, Astronomy, 16, 6
Danner, R., & Unwin, S. 1999, *SIM*: Taking the Measure of the Universe (Pasadena: JPL)
de Felice, F., Bucciarelli, B., Lattanzi, M. G., & Vecchiato, A. 2001, A&A, 373, 336
de Felice, F., Crosta, M. T., Vecchiato, A., Lattanzi, M. G., & Bucciarelli, B. 2004, ApJ, 607, 580
de Felice, F., Lattanzi, M. G., Vecchiato, A., & Bernacca, P. L. 1998, A&A, 332, 1133
Dekany, R., Angel, R., Hege, K., & Wittman, D. 1994, Ap&SS, 212, 299
Deming, D., Seager, S., Richardson, L. J., & Harrington, J. 2005, Nature, 434, 740
Derie, F., Delplancke, F., Glindemann, A., Lévêque, S., Ménardi, S., Paresce, F., Wilhelm, R., & Wirenstrand, K. 2003, in GENIE-DARWIN Workshop, Hunting for Planets (ESA SP-522; Noordwijck: ESA), 61
Des Marais, D. J., et al. 2002, Astrobiology, 2, 153
Doroshenko, O. V., & Kopeikin, S. M. 1995, MNRAS, 274, 1029
Dorren, J. D. 1987, ApJ, 320, 756
Dravins, D., Lindegren, L., & Madsen, S. 1999, A&A, 348, 1040
Eaton, J. A., Henry, G. W., & Fekel, F. C. 1996, ApJ, 462, 888
Eggenberger, A., Udry, S., & Mayor, M. 2004, A&A, 417, 353
Eisner, J. A., & Kulkarni, S. R. 2001, ApJ, 561, 1107
———. 2002, ApJ, 574, 426
Eker, Z. 1994, ApJ, 420, 373
Fischer, D. A., Marcy, G. W., Butler, R. P., Vogt, S. S., Walp, B., & Apps, K. 2002, PASP, 114, 529
Fischer, D. A., & Valenti, J. 2005, ApJ, 622, 1102
Ford, E. B. 2004, PASP, 116, 1083
Ford, E. B., Seager, S., & Turner, E. L. 2001b, Nature, 412, 885
Ford, E. B., & Tremaine, S. 2003, PASP, 115, 1171
Fortney, J. J., Marley, M. S., Lodders, K., Saumon, D., & Freedman, R. 2005, ApJ, 627, L69
Fredrick, L. W., & Ianna, P. A. 1980, BAAS, 12, 455
Fridlund, C. V. M. 2000, in Darwin and Astronomy: The Infrared Space Interferometer (ESA-SP 451; Noordwijck: ESA), 11
Gai, M., Carollo, D., Delbò, M., Lattanzi, M. G., Massone, G., Bertinetto, F., Mana, G., & Cesare, S. 2001, A&A, 367, 362
Gatewood, G. D. 1974, AJ, 79, 52

Gatewood, G. D. 1987, AJ, 94, 213
———. 1991, BAAS, 23, 1433
———. 1995, Ap&SS, 223, 91
———. 1996, BAAS, 28, 885
Gatewood, G. D., & Eichhorn, H. 1973, AJ, 78, 769
Gatewood, G. D., Han, I., & Black, D. C. 2001, ApJ, 548, L61
Gatewood, G. D., Stein, J., de Jonge, J. K., Persinger, T., Reiland, T., & Stephenson, B. 1992, AJ, 104, 1237
Gaudi, B. S., Seager, S., & Mallén-Ornelas, G. 2005, ApJ, 623, 472
Glindemann, A., et al. 2003, Ap&SS, 286, 35
Goldreich, P., & Soter, S 1966, Icarus, 5, 375
Goldreich, P., & Tremaine, S. 1979, ApJ, 233, 857
Goldreich, P., & Tremaine, S. 1980, ApJ, 241, 425
Gonzalez, G. 1998, in ASP Conf. Ser. 134, Brown Dwarfs and Extrasolar Planets, ed. R. Rebolo, E. L. Martin & M. R. Zapatero Osorio (San Francisco: ASP), 431
———. 2003, Rev. Mod. Phys., 75, 101
Gould, A. 2001, ApJ, 559, 484
Goździewski, K., & Konacki, M. 2004, ApJ, 610, 1093
Green, R. 1985, Spherical Astronomy (Cambridge: Cambridge Univ. Press)
Grießmeier, J.-M., et al. 2004, A&A, 425, 753
Gu, P.-G., Bodenheimer, P. H., & Lin, D. N. C. 2004, ApJ, 608, 1076
Gu, P.-G., Lin, D. N. C., & Bodenheimer, P. H. 2003, ApJ, 588, 509
Gubler, J., & Tytler, D. 1998, PASP, 110, 738
Guillot, T. 2005, Annu. Rev. Earth Planet. Sci., 33, 493
Halbwachs, J. L., Mayor, M., & Udry, S. 2005, A&A, 431, 1129
Han, I. 1989, AJ, 97, 607
Han, I., Black, D. C., & Gatewood, G. D. 2001, ApJ, 548, L57
Harrington, R. S. 1986, BAAS, 18, 912
Harrington, R. S., & Harrington, B. J. 1987, Mercury, 16, 77
Heintz, W. D. 1976, MNRAS, 175, 533
Hellings, L. W. 1986, AJ, 91, 650
Henry, G. W., Marcy, G. W., Butler, R. P., & Vogt, S. S. 2000, ApJ, 529, L41
Hershey, J. L. 1973, AJ, 78, 421
Hershey, J. L., & Lippincott, S. L. 1982, AJ, 87, 840
Holman, M. J., & Murray, N. W. 2005, Science, 307, 1288
Holman, M. J., & Wiegert, P. A. 1999, AJ, 117, 621
Horne, J. H., & Baliunas, S. L. 1986, ApJ, 302, 757
Hufnagel, R. E. 1974, Optical Propagation through Turbulence OSA Technical Digest Series, paper WA1 (Washington, D. C.: Opt. Soc. Am.)
Hummel, C. A., Armstrong, J. T., Quirrenbach, A., Buscher, D. F., Mozurkewich, D., Elias, N. M., II, & Wilson, R. E. 1994, AJ, 107, 1859
Ida, S., & Lin, D. N. C. 2004a, ApJ, 604, 388
———. 2004b, ApJ, 616, 567
———. 2005, ApJ, 626, 1045
Jensen, O. G., & Ulrych, T. 1973, AJ, 78, 1104
Ji, J., Liu, L., Kinoshita, H., Zhou, J., Nakai, H., & Li, G. 2003, ApJ, 591, L57
Jones, B. W., Underwood, D. R., & Sleep, P. N. 2005, ApJ, 622, 1091
Kasting, J. F., Whitmire, D. P., & Reynolds, R. T. 1993, Icarus, 101, 108
Kells, L. M., Kern, W. F., & Bland, J. R. 1942, Spherical Trigonometry with Naval and Military Applications (New York: McGraw-Hill)
Kiseleva-Eggleton, L., Bois, E., Rambaux, N., & Dvorak, R. 2002, ApJ, 578, L145
Kley, W. 2000, MNRAS, 313, L47
———. 2001, in Proc. IAU Symp. 200, The Formation of Binary Stars, ed. H. Zinnecker & R. D. Mathieu (San Francisco: ASP), 511
Kley, W., & Burkert, A. 2000, in ASP Conf. Ser. 219, Disks, Planetesimals, and Planets, ed. F. Garzón, C. Eiroa, D. de Winter, & T. J. Mahoney (San Francisco: ASP), 189
Klioner, S. A. 2003, AJ, 125, 1580
———. 2004, Phys. Rev. D, 69, 124001
Klioner, S. A., & Kopeikin, S. M. 1992, AJ, 104, 897
Konacki, M., Maciejewski, A. J., & Wolszczan, A. 2002, ApJ, 567, 566
Konacki, M., Torres, G., Jha, S., & Sasselov, D. D. 2003, Nature, 421, 507
Konacki, M., Torres, G., Sasselov, D. D., & Jha, S. 2005, ApJ, 624, 372
Konacki, M., et al. 2004, ApJ, 609, L37
Kopeikin, S. M., Schäfer, G., Gwinn, C. R., & Eubanks, T. M. 1999, Phys. Rev. D, 59, 84023
Kornet, K., Bodenheimer, P., Rózyczka, M., & Stepinski, T. F. 2005, A&A, 430, 1133
Kovalevsky, J. 1980, Celest. Mech., 22 153
———. 2002, Modern Astrometry (2nd ed.; Berlin: Springer)
Kovalevsky, J., & Seidelmann, P. K. 2004, Fundamentals of Astrometry (Cambridge: Cambridge Univ. Press)
Kürster, M., et al. 2003, A&A, 403, 1077
Lammer, H., Selsis, F., Ribas, I., Guinan, E. F., Bauer, S. J., & Weiss, W. W. 2003, ApJ, 598, L121
Lane, B. F., & Colavita, M. M. 2003, AJ, 125, 1623
Lane, B. F., Colavita, M. M., Boden, A. F., & Lawson, P. R. 2000, Proc. SPIE, 4006, 452
Lane, B. F., & Muterspaugh, M. W. 2004, ApJ, 601, 1129
Lattanzi, M. G., Casertano, S., Jancart, S., Morbidelli, R., Pannunzio, R., Pourbaix, D., Sozzetti, A., & Spagna, A. 2005, in *Gaia*: The Three-Dimensional Universe (ESA SP-576; Noordwijck: ESA), 251
Lattanzi, M. G., Casertano, S., Sozzetti, A., & Spagna, A. 2002, in GAIA: A European Space Project, ed. O. Bienaymé & C. Turon, EAS Publications Series (Les Ulis: EDP Sciences), 2, 207
Lattanzi, M. G., Sozzetti, A., & Spagna, A. 2000a, in From Extrasolar Planets to Cosmology: The VLT Opening Symposium, ed. J. Bergeron & A. Renzini (Berlin: Springer), 497
Lattanzi, M. G., Spagna, A., Sozzetti, A., & Casertano, S. 1997, in Proc. ESA Symp., *Hipparcos*, Venice '97, ed. B. Battrick (ESA SP-402; Noordwijk: ESA), 755
———. 2000b, MNRAS, 317, 211
Laughlin, G., Bodenheimer, P., & Adams, F. C. 2004, ApJ, 612, L73
Laughlin, G., Wolf, A., Vanmunster, T., Bodenheimer, P., Fischer, D., Marcy, G. W., Butler, R. P., & Vogt, S. S. 2005, ApJ, 621, 1072
Lawrence, J. S., Ashley, M. C. B., Tokovinin, A., & Travouillon, T. 2004, Nature, 431, 278
Laws, C., et al. 2003, AJ, 125, 2664
Lazorenko, P. F. 2002, A&A, 396, 353
Lazorenko, P. F., & Lazorenko, G. A. 2004, A&A, 427, 1127
Lecavelier des Etangs, A., Vidal-Madjar, A., McConnell, J. C., & Hébrard, G. 2004, A&A, 418, L1
Lin, D. N. C., & Papaloizou, J. C. B. 1993, in Protostars and Planets III, ed. E. H. Levy & J. I. Lunine (Tucson: Univ. Arizona Press), 749
Lindegren, L. 1978, IAU Colloq. 48, Modern Astrometry, ed. F. V. Prochazka & R. H. Tucker (Vienna: Inst. Astron.), 197
Lindegren, L. 1980, A&A, 89, 41
———. 1989, in The *Hipparcos* Mission: Pre-Launch Status, Vol. III (ESA SP-1111, Noordwijck: ESA), 311
Lindegren, L., & Kovalevsky, J. 1989, in The *Hipparcos* Mission: Pre-Launch Status, Vol. III (ESA SP-1111, Noordwijck: ESA), 1
Lineweaver, C. H., & Grether, D. 2003, ApJ, 598, 1350
Lippincott, S. L. 1960, AJ, 65, 349
———. 1960, AJ, 65, 445

Lissauer, J. J. 1993, ARA&A, 31, 129
Livio, M., & Pringle, J. E. 2003, MNRAS, 346, L42
Lloyd, J. P., Oppenheimer, B. R., & Graham, J. R. 2002, PASA, 19, 318
Lomb, N. R. 1976, Ap&SS, 39, 447
Lovelock, J. 1965, Nature, 207, 568
Marcy, G. W., Butler, R. P., Fischer, D. A., & Vogt, S. S. 2004a, in ASP Conf. Ser. 294, Scientific Frontiers in Research on Extrasolar Planets, ed. D. Deming & S. Seager (San Francisco: ASP), 1
———. 2004b, in ASP Conf. Ser. 321, Extrasolar Planets: Today and Tomorrow, ed. J.-P. Beaulieu, A. Lecavelier des Etangs, & C. Terquem (San Francisco: ASP), 3
Marcy, G. W., Fischer, D. A., McCarthy, C., & Ford, E. B. 2005, in ASP Conf. Ser. 338, Astrometry in the Age of the Next Generation of Large Telescopes, ed. P. K. Seidelmann & A. K. B. Monet (San Francisco: ASP), 191
Marzari, F., Weidenschilling, S., Barbieri, M., & Granata, V. 2005, ApJ, 618, 502
Mayer, L., Quinn, T., Wadsley, J., & Stadel, J. 2002, Science, 298, 1756
———. 2004, ApJ, 609, 1045
———. 2005, MNRAS, submitted (astro-ph/0405502)
Mayor, M., & Queloz, D. 1995, Nature, 378, 355
Mayor, M., Udry, S., Naef, D., Pepe, F., Queloz, D., Santos, N. C., & Burnet, M. 2004, A&A, 415, 391
Mazeh, T., & Zucker, S. 2003, ApJ, 590, L115
Mazeh, T., Zucker, S., dalla Torre, A., & van Leeuwen, F. 1999, ApJ, 522, L149
Mazeh, T., et al. 2000, ApJ, 532, L55
McArthur, B. E., et al. 2004, ApJ, 614, L81
McGrath, M. A., et al. 2002, ApJ, 564, L27
———. 2004, in ASP Conf. Ser. 294, Scientific Frontiers in Research on Extrasolar Planets, ed. D. Deming & S. Seager (San Francisco: ASP), 145
Menou, C., & Tabachnik, S. 2003, ApJ, 583, 473
Miralda-Escudé, J. 2002, ApJ, 564, 1019
Monet, D. G. 1979, ApJ, 234, 275
Monet, D. G., Dahn, C. C., Vrba, F. J., Harris, H. C., Pier, J. R., Luginbuhl, C. B., & Ables, H. D. 1992, AJ, 103, 638
Moutou, C., Pont, F., Bouchy, F., & Mayor, M. 2004, A&A, 424, L31
Musielak, Z. E., Cuntz, M., Marshall, E. A., & Stuit, T. D. 2005, A&A, 434, 355
Naef, D., Mayor, M., Beuzit, J. L., Perrier, C., Queloz, D., Sivan, J. P., & Udry, S. 2005, in XIII Cambridge Workshop on Cool Stars, Stellar Systems, and the Sun (ESA-SP 560; Noordwijck: ESA), in press
Naef, D., et al. 2001, A&A, 375, L27
Neat, G. W., Abramovici, A. R., Calvet, R. J., Korechoff, R. P., Joshi, S. S., & Goullioud, R. 1998, Proc. SPIE 3350, 1020
Nelson, A. F. 2000, ApJ, 537, L65
———. 2003, MNRAS, 345, 233
Oppenheimer, B. R., Kulkarni, S. R., & Stauffer, J. R. 2000, in Protostars and Planets IV, ed V. Mannings, A. P. Boss, & S. S. Russell (Tucson: Univ. Arizona Press), 1313
Papaloizou, J. C. B., & Terquem, C. 2001, MNRAS, 325, 221
Pätzold, M., & Rauer, H. 2002, ApJ, 568, L117
Perryman, M. A. C., et al. 1996, A&A, 310, L21
———. 1997, A&A, 323, L49
———. 2001, A&A, 369, 339
Pilat-Lohinger, E., Funk, B., & Dvorak, R. 2003, A&A, 400, 1085
Pollack, J. B., Hubickyj, O., Bodenheimer, P., Lissauer, J. J., Podolack, M., & Greenzweig, Y. 1996, Icarus, 124, 62
Pont, F., Bouchy, F., Queloz, D., Santos, N. C, Melo, C., Mayor, M., & Udry, S. 2004, A&A, 426, L15
Pourbaix, D. 2001, A&A, 369, L22
———. 2002, A&A, 385, 686
Pourbaix, D., & Arenou, F. 2001, A&A, 372, 935
Pourbaix, D., & Jorissen, A. 2000, A&AS, 145, 161
Pravdo, S. H., & Shaklan, S. B. 1996, ApJ, 465, 264
Press, W. H., et al. 1992, Numerical Recipes in FORTRAN: the Art of Scientific Computing (Cambridge: Cambridge Univ. Press)
Queloz, D., et al. 2000, A&A, 354, 99
Quirrenbach, A., Mozurkewich, D., Buscher, D. F., Hummel, C. A., & Armstrong, J. T. 1994, A&A, 286, 1019
Rafikov, R. R. 2005, ApJ, 621, L69
Raymond, S. N., & Barnes, R. 2005, ApJ, 619, 549
Raymond, S. N., Quinn, T., & Lunine, J. I. 2004, Icarus, 168, 1
Rice, W. K. M., Armitage, P. J., Bate, M. R., & Bonnell, I. A. 2003a, MNRAS, 339, 1025
———. 2003b, MNRAS, 338, 227
Rice, W. K. M., Armitage, P. J., Bonnell, I. A., Bate, M. R., Jeffers, S. V., & Vine, S. G. 2003c, MNRAS, 346, L36
Santos, N. C., Israelian, G., & Mayor, M. 2001, A&A, 373, 1019
———. 2004a, A&A, 415, 1153
Santos, N. C., Israelian, G., Mayor, M., Rebolo, R., & Udry, S. 2003, A&A, 398, 363
Santos, N. C., et al. 2004b, A&A, 426, L19
Scargle, J. D. 1982, ApJ, 263, 835
Schilling, G. 1985, Astronomy, 13, 26
Schroeder, D. J., et al. 2000, AJ, 119, 906
Schuessler, M., Caligari, P., Ferriz-Mas, A., Solanki, S. K., & Stix, M. 1996, A&A, 314, 503
Seager, S., & Ford, E. B. 2005, in STScI Symp. Ser. 16, Astrophysics of life, ed. M. Livio, I. N. Reid, & W. B. Sparks (Cambridge: Cambridge Univ. Press), 67
Selsis, F., Despois, D., & Parisot, J.-P. 2002, A&A, 388, 985
Shaklan, S. B., et al. 1998, Proc. SPIE, 3350, 1009
Shao, M., Boden, A. F., Colavita, M. M., Lane, B. F., & Lawson, P. R. 1999, BAAS, 31, 1504
Shao, M., & Colavita, M. M. 1992, A&A, 262, 353
Shao, M., Colavita, M. M., Hines, B. E., Staelin, D. H., & Hutter, D. J. 1988, A&A, 193, 357
Shao, M., et al. 1990, AJ, 100, 1701
Soffel, M. H. 1989, Relativity in Astrometry, Celestial Mechanics, and Geodesy (Berlin: Springer)
Sozzetti, A. 2004, MNRAS, 354, 1194
Sozzetti, A., Casertano, S., Brown, R. A., & Lattanzi, M. G. 2002, PASP, 114, 1173
———. 2003a, PASP, 115, 1072
Sozzetti, A., Casertano, S., Lattanzi, M. G., & Spagna, A. 2001, A&A, 373, L21
———. 2003b, in Towards Other Earths: DARWIN/TPF and the Search for Extrasolar Terrestrial Planets, ed. M. Fridlund & T. Henning (ESA SP-539; Noordwijck: ESA), 605
Sozzetti, A., Latham, D. W., Torres, G., Stefanik, R. P., Boss, A. P., Carney, B. W., & Laird, J. B. 2005, in *Gaia*: The Three-Dimensional Universe (ESA-SP 576; Noordwijck: ESA), 309
Sozzetti, A., Spagna, A., & Lattanzi, M. G. 2000, Earth Moon Planets, 81, 103
Sozzetti, A., et al. 2004, ApJ, 616, L167
Stairs, I. H., Arzoumanian, Z., Camilo, F., Lyne, A. G., Nice, D. J., Taylor, J. H., Thorsett, S. E., & Wolszczan, A. 1998, ApJ, 505, 352
Stairs, I. H., Thorsett, S. E., Taylor, J. H., & Wolszczan, A. 2002, ApJ, 581, 501
Tabachnik, S., & Tremaine, S. 2002, MNRAS, 335, 151
Taff, L. G. 1990, ApJ, 365, 407

Takeuchi, T., Velusamy, T., & Lin, D. N. C. 2005, ApJ, 618, 987
Terquem, C. 2003, in Planetary Systems and Planets in Systems, ed. S. Udry, W. Benz, & R. von Steiger (ISSI Space Sci. Ser. 19; Dordrecht: Kluwer)
Terquem, C., & Papaloizou, J. C. B. 2002, MNRAS, 332, 39
Thébault, P., Marzari, F., & Scholl, H. 2002, A&A, 384, 594
Torres, G., Konacki, M., Sasselov, D. D., & Jha, S. 2004, ApJ, 609, 1071
Tremaine, S., & Zakamska, N. L. 2004, in AIP Conf. Proc. 713, The Search for Other Worlds: XIV Astrophysics Conference, ed. S. S. Holt & D. Deming (New York: AIP), 243
Trilling, D. E., Benz, W., Guillot, T., Lunine, J. I., Hubbard, W. B., & Burrows, A. 1998, ApJ, 500, 428
Trilling, D. E., Lunine, J. I., & Benz, W. 2002, A&A, 394, 241
Udalski, A., Pietrzynski, G., Szymanski, M., Kubiak, M., Zebrun, K., Soszynski, I., Szewczyk, O., & Wyrzykowski, L. 2003, Acta Astron., 53, 133
Udalski, A., Zebrun, K., Szymanski, M., Kubiak, M., Soszynski, I., Szewczyk, O., Wyrzykowski, L., & Pietrzynski, G. 2002a, Acta Astron., 52, 115
Udalski, A., et al. 2002b, Acta Astron., 52, 1
Udry, S., Mayor, M., Naef, D., Pepe, F., Queloz, D., Santos, N. C., & Burnet, M. 2002, A&A, 390, 267
Udry, S., Mayor, M., & Santos, N. C. 2003, A&A, 407, 369
van Belle, G. T., Boden, A. F., Colavita, M. M., Shao, M., Vasisht, G., & Wallace, J. K. 1998, Proc. SPIE, 3350, 362
van de Kamp, P. 1963, AJ, 68, 515
———. 1969a, AJ, 74, 238
———. 1969b, AJ, 74, 757
———. 1975, AJ, 80, 658
———. 1982, Vistas Astron., 26, 141
Vecchiato, A., Lattanzi, M. G., Bucciarelli, B., Crosta, M., de Felice, F., & Gai, M. 2003, A&A, 399, 337
Vidal-Madjar, A., Lecavelier des Etangs, A., Désert, J.-M., Ballester, G. E., Ferlet, R., Hébrard, G., & Mayor, M. 2003, Nature, 422, 143
Vidal-Madjar, A., et al. 2004, ApJ, 604, L69
Ward, W. R. 1986, Icarus, 67, 164
———. 1997, ApJ, 482, L211
Will, C. M. 1993, Theory and Experiment in Gravitational Physics (rev. ed.; Cambridge: Cambridge Univ. Press)
Wolszczan, A., & Frail, D. A. 1992, Nature, 355, 145
Woolf, N., & Angel, J. R. 1998, ARA&A, 36, 507
Wyant, J. C. 1975, Appl. Opt., 14, 2622
Zucker, S., & Mazeh, T. 2000, ApJ, 531, L67
———. 2001a, ApJ, 562, 1038
———. 2001b, ApJ, 562, 549
———. 2002, ApJ, 568, L113